Aus der Klinik für Infektiologie und Mikrobiologie
der Universität zu Lübeck
Direktor: Prof. Dr. Jan Rupp

Genetische Modifikation von *Chlamydia pneumoniae*

Inauguraldissertation
zur
Erlangung der Doktorwürde
der Universität zu Lübeck
- Aus der Sektion Medizin -

vorgelegt von
Maximilian Wanker
aus Heilbronn

Lübeck 2022

1. Berichterstatter: Prof. Dr. med. Jan Rupp

2. Berichterstatterin: Prof. Dr. rer. nat. Katja Lohmann

Tag der mündlichen Prüfung: 25.05.2022

Zum Druck genehmigt. Lübeck, den 25.05.2022

Promotionskommission der Sektion Medizin

Table of contents

1 List of abbreviations

Table 1: Aberrations used in this thesis in alphabetic order.

°C	Degree Celsius
µL	Microliter
µm	Micrometer
A. dest.	Distilled water (Latin: Aqua destillata)
AB	Aberrant body
ABs	Aberrant bodies
BLAST	Basic Local Alignment Search Tool
bp	Base pair
BSA	Bovine Serum Albumin
C.	*Chlamydia*
CAD	Coronary artery disease
CAM	Chloramphenicol
CAP	Community-acquired pneumonia
CAT	Chloramphenicol acetyltransferase
CDS	Coding DNA sequence
cf.	Compare (abbreviation from Latin: “conferatur”)
COPD	Chronic obstructive pulmonary disease
Cpn	*Chlamydia pneumoniae*
CV	Cardiovascular
DMEM	Dulbecco's Modified Eagle's Medium
DNA	Deoxyribonucleic acid
dNTP	Deoxyribonucleoside triphosphate
Dr.	Doctor
DZIF	Deutsches Zentrum für Infektionsforschung e. V.
E.	*Escherichia*
e.g.	For example (abbreviation from Latin: “exempli gratia”)
EB	Elementary body
EBs	Elementary bodies
EDTA	Ethylenediaminetetraacetic acid
et al.	Latin: and others
FITC	Fluorescein isothiocyanate
h	Hour
h.p.i.	Hours post infection
HEp-2 cells	Human epithelial type 2 cells
L	Liter
LB	Lysogeny broth (1)
LN_2	Liquid nitrogen
M.D.	Doctor of Medicine (abbreviation from Latin: “Medicinae Doctor”)
Mb	Mega base
MCIP	Meningococcal class I protein promoter
min	Minute
mL	Milliliter
NCBI	National Center for Biotechnology Information
nm	Nanometer
No.	Number

NOX	Normoxia
nsSNP	Non-synonymous single-nucleotide polymorphism
OD	Optical density
PBS	Phosphate buffered saline
PCR	Polymerase chain reaction
PD	Privatdozent
Prof.	Professor
RB	Reticulate body
RBs	Reticulate bodies
RSGFP	Red-shifted green fluorescent protein
sec	Second
SNP	Single-nucleotide polymorphism
sSNP	Synonymous single-nucleotide polymorphism
TEM	Transmission electron microscopy
Tris	Tris(hydroxymethyl)aminomethane
tyrP	Tyrosine/tryptophan permease

2 Abstract

Chlamydia pneumoniae (*C. pneumoniae*) are obligate intracellular Gram-negative bacteria. They infect lung epithelial cells and alveolar macrophages, which leads to atypical community-acquired pneumonia (CAP) in humans. *C. pneumoniae* is also associated with chronic respiratory diseases such as asthma and chronic obstructive pulmonary disease (COPD). There is also growing evidence that *C. pneumoniae* is strongly associated with cardiovascular diseases such as atherosclerosis. In addition to strains that are contagious to humans, some *C. pneumoniae* strains also infect animals and cause various respiratory and genitourinary diseases. Although much is known about chlamydial infections and related diseases, the lack of tools to genetically modify *C. pneumoniae* has greatly hindered further research of this unique pathogen. Conventional transformation protocols for chlamydiae that use a plasmid shuttle vector are not applicable to *C. pneumoniae*. Therefore, we developed a new *C. pneumoniae*-derived plasmid shuttle vector called pRSGFP-CAT-Cpn. As well as the chlamydial backbone from *C. pneumoniae* N16, this new plasmid shuttle vector contains the red-shifted green fluorescent protein (RSGFP) gene and the chloramphenicol acetyltransferase (CAT) gene. Using this new shuttle vector, we successfully transformed not only animal isolate *C. pneumoniae* LPCoLN but also human isolate *C. pneumoniae* CV-6. Subsequent studies showed that pRSGFPCAT-Cpn had no significant effect on the morphological and growth characteristics of chlamydiae. Furthermore, we demonstrated that antibiotic selection pressure is not necessary to ensure the stability of pRSGFPCAT-Cpn during incubation. Additionally, taxonomically close relatives of *C. pneumoniae* named *C. felis* [*C. felis* Not Identified (N.I.), *C. felis* 02DC26 (Cf02-23), and *C. felis* Cello] were successfully transformed with pRSGFPCAT-Cpn, suggesting that pRSGFPCAT-Cpn can overcome the barrier between chlamydial species caused by the plasmid tropism phenomenon. According to our results, the novel plasmid shuttle vector pRSGFPCAT-Cpn is a well-functioning and promising new genetic tool for future chlamydial research.

Zusammenfassung

Chlamydia pneumoniae (*C. pneumoniae*) sind obligat intrazelluläre lebende gramnegative Bakterien. Sie infizieren Lungenepithelzellen und Alveolarmakrophagen, welches beim Menschen zu einer atypischen ambulant erworbenen Lungenentzündung [community-acquired pneumonia (CAP)] führen kann. *C. pneumoniae* werden auch mit chronischen Atemwegserkrankungen wie Asthma und der chronisch obstruktiven Lungenerkrankung [chronic obstructive pulmonary disease (COPD)] in Verbindung gebracht. Des Weiteren gibt es auch Hinweise, dass *C. pneumoniae* Einflüsse auf die Entstehung von Herz-Kreislauf-Erkrankungen wie zum Beispiel Atherosklerose haben. Neben diesen humanpathogenen *C. pneumoniae* Stämmen gibt es aber auch einige Stämme, die Tiere infizieren und hierbei Infektionen des Atem-, aber auch des Urogenitaltrakts verursachen. Obwohl viel über Chlamydien und die damit verbundenen Krankheiten bekannt ist, hat der Mangel an Werkzeugen zur genetischen Veränderung von *C. pneumoniae* die weitere Erforschung dieser einzigartigen Erreger stark eingeschränkt. Herkömmliche Transformationsprotokolle für Chlamydien, die einen Plasmid-Shuttle-Vektor verwenden, sind nicht für *C. pneumoniae* verfügbar. Daher widmete sich diese Arbeit der Entwicklung eines neuen Plasmid-Shuttle-Vektors namens pRSGFPCAT-Cpn, welcher neben Bestandteilen des Plasmids von *C. pneumoniae* N16 auch das Gen für das *red-shifted green fluorescent protein (RSGFP)* und das Gen für die *chloramphenicol acetyltransferase (CAT)* enthält. Mit diesem neuen Plasmid-Shuttle-Vektor war es möglich *C. pneumoniae* LPCoLN, aber auch *C. pneumoniae* CV-6 erfolgreich zu transformieren. Weitere Experimente zeigten, dass pRSGFPCAT-Cpn keine Auswirkungen auf die Morphologie und das Wachstum von *C. pneumoniae* hatte. Auch konnte gezeigt werden, dass kein antibiotischer Selektionsdruck notwendig ist, um die Präsenz von pRSGFPCAT-Cpn zu gewährleisten. In anschließenden Experimenten konnte pRSGFPCAT-Cpn auch für die Transformation von *C. felis* [*C. felis* Not Identified (N.I.), *C. felis* 02DC26 (Cf02-23) und *C. felis* Cello], taxonomisch nahe Verwandte von *C. pneumoniae,* genutzt werden. Dies deutet darauf hin, dass pRSGFPCAT-Cpn die Barriere zwischen den verschiedenen Arten von Chlamydien, welche als Plasmid Tropismus beschrieben wurde, überwinden kann. Der neuartige Plasmid-Shuttle-Vektor pRSGFPCAT-Cpn ist daher ein sehr gut funktionierendes und vielversprechendes gentechnisches Werkzeug für zukünftige Chlamydienforschung.

3 Introduction

3.1 Chlamydiae

3.1.1 Chlamydial developmental life cycle

The Gram-negative *Chlamydia* spp. are obligate intracellular bacteria which depend on their host's metabolism. Due to this, they share an inimitable biphasic developmental life cycle. They alternate between the infectious elementary bodies (EBs) and the metabolically active and replicating reticulate bodies (RBs) (2–4). During stress exposure, chlamydiae can also switch into the protective persistent form and differentiate into so-called aberrant bodies (ABs). After removal of stress exposure, chlamydiae can re-enter the developmental life cycle (cf. figure 1).

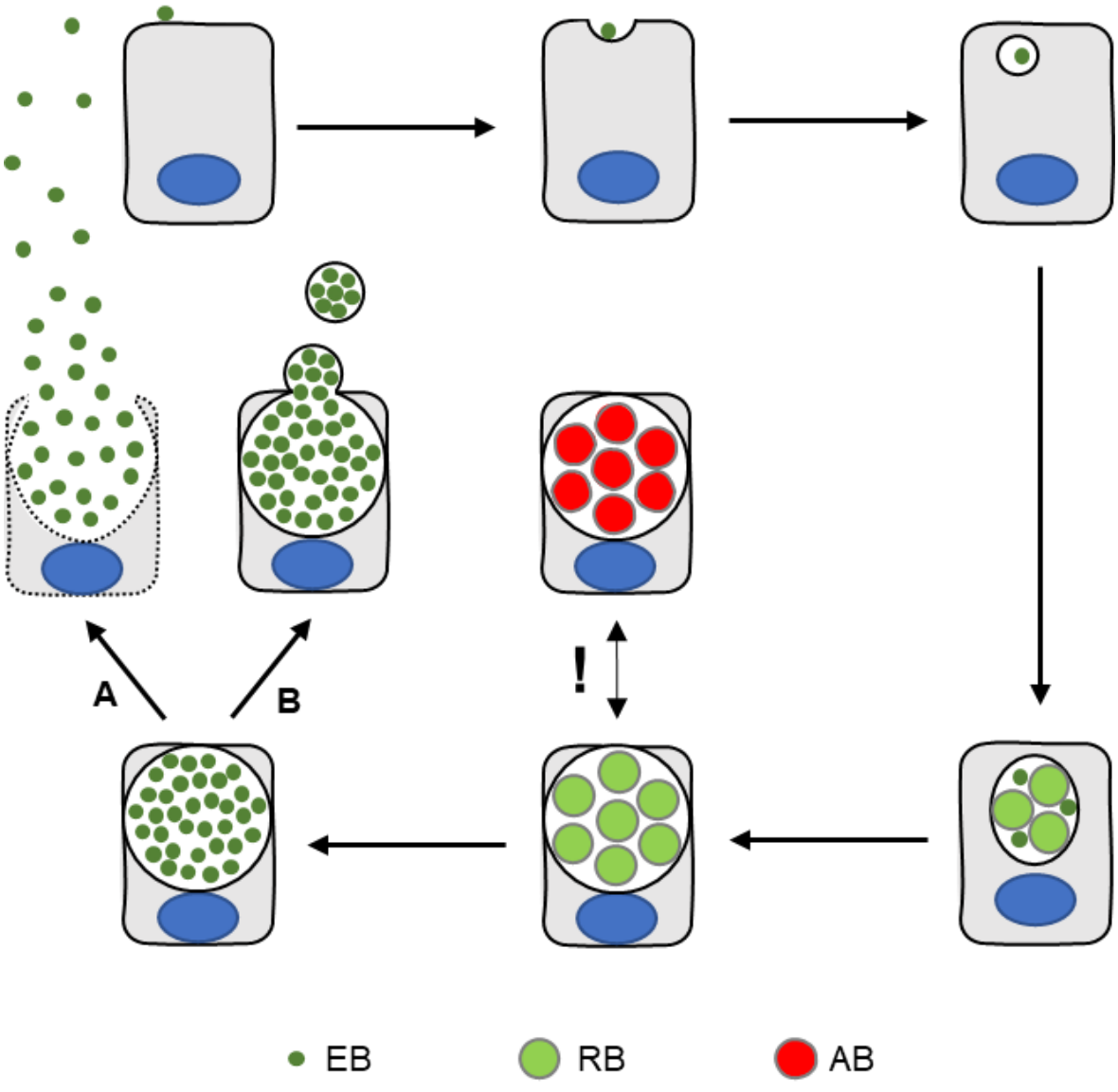

Figure 1: Chlamydial developmental life cycle.
EBs infect host cell. After the EB is entering the host cell it builds the chlamydial inclusion and differentiate into the RB. After replication, a second differentiation takes place and RBs further differentiate into EBs. Finally, chlamydiae leave the host cell via cell lysis (dotted line) (A) or via extrusion (B) and infect new host cells. During stress exposure (exclamation point) persistent form is induced and chlamydiae differentiate into ABs. After elimination of stress factors, chlamydiae are still able to continue their developmental life cycle. Nucleus of host cell is represented in blue.

3.1.1.1 Elementary body

The approximately 0.3 µm EBs are the infectious form of chlamydiae. Due to their robust cell wall, EBs are resistant to osmotic and mechanic stress. Cysteine rich proteins within their cell wall leading to the development of disulfide bonds guaranteeing its stability (3–5). Although EBs have reduced metabolism, they can use D-glucose-6-phosphate to generate energy (6). Proteome analysis of chlamydial EBs reveals that they express metabolic related proteins needed for glucose metabolism. It is suggested that glycolytic activity might be needed for host cell entry and for the differentiation into RBs (7). It is known that EBs interact with host cell receptors e.g. heparan sulfate proteoglycans (HSPGs) which might be related to chlamydial tissue specificity. This phenomenon is called tissue tropism (5).

When EBs have interacted with the host cell surface, effector molecules are injected via pre-synthesized type III secretion systems (T3SS) into the cytoplasm. After entering the host cell, chlamydiae develop the so-called chlamydial inclusion, a detached chlamydial compartment within the host cell. After approximately 8 hours post infection (h.p.i.) EBs start to differentiate into the replicating and metabolic active form called RBs (8).

3.1.1.2 Reticulate body

Compared to EBs, the non-infectious RBs are larger (ca. 1.0 µm) and more metabolically active. RBs are essential for chlamydial nutrition purchase and replication (3–5). However, RBs still depend on host metabolism due to their truncated metabolic pathways. Therefore, chlamydiae interact with host cell organelles such as the Golgi apparatus to acquire metabolites from the host cell (3,9,10).

Approximately 19 h after initial infection, RBs start to replicate and after 48 h.p.i. the re-differentiation into infectious EBs begins. Finally, after approximately 84 h.p.i.,

chlamydiae initiate host cell lysis (cf. figure 1A) or extrusion (cf. figure 1B) to infect new host cells (20) (cf. figure 1).

3.1.1.3 Persistent form

When the infected host cell is exposed to stress stimuli chlamydiae can pause their developmental life cycle and switch into the non-cultivable persistent form and build ABs to guarantee their survival during stress exposure (3,11). Chlamydiae switch into the persistent form when the infected host cell is exposed to stress stimuli such as antibiotics (e.g. penicillin) (12–14), interferon gamma (IFN-γ) (15), adenosine (16), lack of essential nutrients including iron, amino acids or glucose (17), heat-shock (15), tobacco smoke (18), infections with chlamydial bacteriophages (19), co-infection with human herpes virus (HHV) (20,21) or porcine epidemic diarrhea virus (PEDV) (22). In absence of the triggering stress stimuli, chlamydiae can re-enter their developmental life cycle and can continue replication using host cell metabolism again. The persistent form of chlamydiae might be associated with chronic diseases. In recent studies, ABs of *C. pneumoniae* were detected not only in human isolated coronary atheromatous heart tissue (23) but also in monocytes (24). After antibiotic treatment, chlamydiae might be recover causing perseverative chronic diseases (11). ABs could also be found in tissue that is infected by *Chlamydia trachomatis* (*C. trachomatis*), *Chlamydia suis* (*C. suis*) and *Chlamydia muridarum* (*C. muridarum*) (25–28).

3.1.2 Taxonomy

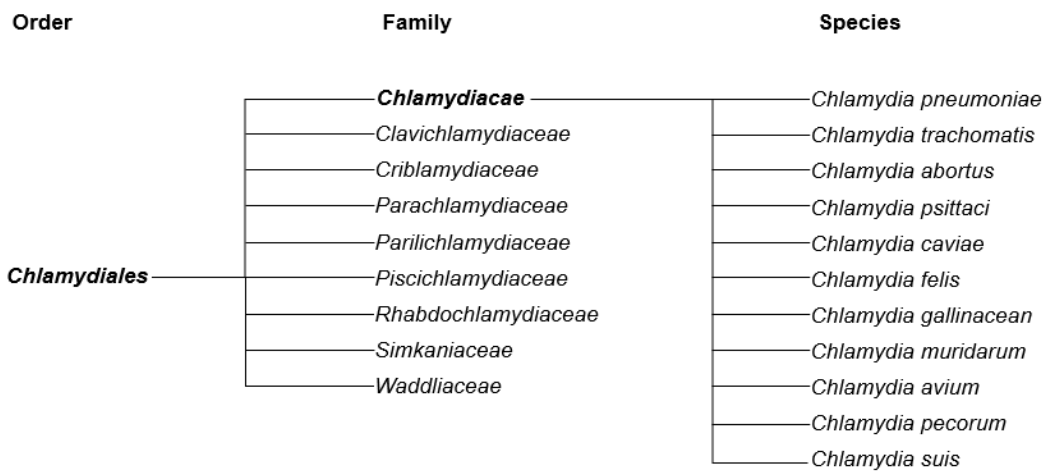

Figure 2: Taxonomic overview of the order *Chlamydiales.*
Phylogenetic relationship is not represented by the length of lines.

Chlamydia spp. belong to the order of *Chlamydiales* (2–4). Due to the DNA sequence of the 16S rRNA, the order of *Chlamydiales* itself can be divided into nine families (2) called the *Chlamydiaceae* family, *Clavichlamydiaceae* family, *Criblamydiaceae* family, *Parachlamydiaceae* family, *Parilichlamydiaceae* family, *Piscichlamydiaceae* family, *Rhabdochlamydiaceae* family, *Simkaniaceae* family and the *Waddliaceae* family. The best investigated representative of the *Chlamydiales* is the family of *Chlamydiaceae* including 11 species (29) named *Chlamydia pneumoniae* (30,31), *Chlamydia trachomatis* (31), *Chlamydia abortus* (31,32), *Chlamydia avium* (31,33), *Chlamydia caviae* (31,34), *Chlamydia felis* (31,32), *Chlamydia gallinacean* (31,33), *Chlamydia muridarum* (31,34), *Chlamydia psittaci* (31), *Chlamydia pecorum* (31,35) and *Chlamydia suis* (31,34) (cf. figure 2).

There are also reports on chlaymdiae species called *Chlamydia ibidis* (31,36) and *Chlamydia buteonis* (31,37). However, those chlamydial strains are not yet listed in the "List of Prokaryotic names with Standing in Nomenclature" (38,39).

In 1999 the family of *Chlamydiaceae* was classified into the genus *Chlamydia* and *Chlamydophila* by Everett *et al.* (34). This new classification, however, was discussed highly controversially among scientists, resulting in reunification of both genus into a single genus called *Chlamydia* (40). In accordance to the results of Schachter *et al.* (41), the use of single genus *Chlamydia* is now commonly used. This thesis primarily focuses on *C. pneumoniae*.

3.1.3 *Chlamydia sp.* cause a variety of diseases

The obligate intracellular pathogen called *C. pneumoniae* infects the respiratory tract and are also associated with cardiovascular diseases in human (42). First human samples were isolated from the conjunctiva of a child in Taiwan within the scope of a trachoma vaccine study in 1965 (43). In 1985 it was erroneously classified as a new strain of *C. psittaci* called TWAR (44,45). The name TWAR was derived from the two first isolated strains called TW-183 and AR-39 (44). In 1989 the erroneous classification as *C. psittaci* was adjusted and the newly discovered *Chlamydia* spp. were reclassified as a new human infecting species of the family of *Chlamydiaceae* called *C. pneumoniae* (30).

Apart from *C. pneumoniae,* there is another human infecting species called *C. trachomatis.* Serotypes A–C of *C. trachomatis* cause infections of the eyes (Trachoma). Other serotypes of *C. trachomatis* cause the most common bacterial sexually transmitted diseases (STDs) globally (3,46,47). For example, serotypes D–K and serotypes L1–L3 cause pelvic inflammatory diseases and Lymphogranuloma venereum in the urogenital tract, respectively. Considering the different clinical pictures of *C. trachomatis* and *C. pneumoniae* it is not surprising that these two human-infecting *Chlamydia* spp. have several distinctions on genome level (48).

Upon closer inspection of *C. pneumoniae* isolated from different human tissues (respiratory tract or coronary arteries), genetic differences have also been elucidated. Although all human isolates of *C. pneumoniae* have a high genome sequence homology, they could be distinguished into three phylogenic clusters. Cluster I contains *C. pneumoniae* TW183 and UZG, cluster II contains YK41, CM1, AR39, GiD and J138 and cluster III contains H12, Panola, K7, U1271, CWL011, CWL029, CWL029c, Wien1, Wien2, Wien3, MUL2216, CV15, CV14, PB1 and PB2 (49,50). It has been suggested that some genetic factors might play an important role for the tissue specificity of chlamydiae during infection, called tissue tropism (49). For instance, the gene copy number of a tyrosine/tryptophan permease (*tyrP*) varies between respiratory and vascular isolated *C. pneumoniae* strains. While respiratory isolates contain several copies of the *tyrP* gene, the majority of vascular isolates stand out with just a single copy (49,51). Furthermore, recent studies show that single-nucleotide polymorphisms (SNPs) in *C. pneumoniae* genome can be used for a more precisely classification of respiratory tract isolates and vascular isolates (49). The location of SNPs found on chlamydial chromosome correlates with the genes responsible for chlamydial RB-to-EB differentiation, inclusion membrane development, chlamydial stress response, or metabolism. These findings could be explain the mechanism of tissue tropism in *C. pneumoniae* (49). These SNP analyses also leading to the idea that human infecting *C. pneumoniae* might be evolved from zoonic *C. pneumoniae* species (52).

Animal isolate *C. pneumoniae* strains were collected from amphibians, reptiles but also mammals such as horses, koalas, or western barred bandicoots (53,54). Apart from infections of the respiratory tract, zoonic *C. pneumoniae* can also cause infections of the ocular or urinogenital system (47,49,52–54).

3.1.4 Pathogenesis of *C. pneumoniae* infections

Human infecting *C. pneumoniae* primarily infect lung epithelial cells and alveolar macrophages of the upper and lower respiratory tract causing 10% of the atypical community-acquired pneumonia (CAP) in adults (55–57). Moreover, *C. pneumoniae* is also associated with chronic respiratory tract diseases such as asthma (58–60) and COPD (61). Since most infected people are asymptomatic, it is not surprising that the prevalence of *C. pneumoniae* IgG antibody already reach 50% in 20-year-olds and about 70-80% in elderly people (62). In addition to infection of the respiratory tract, *C. pneumoniae* also seems to be involved in the pathogenesis of cardiovascular diseases such as atherosclerosis (42,63,64) and coronary artery diseases (CAD) (65,66). A meta-analysis including 16 studies suggests that *C. pneumoniae* is linked to atherosclerosis by promoting inflammatory conditions (67). Several studies showed the presence of *C. pneumoniae* within atherosclerotic tissue using polymerase chain reaction, immunocytochemistry, electron microscopy, immunofluorescence assay, enzyme-linked immunosorbent assay, *in situ* hybridization or bacteriological culture (68). *C. pneumoniae* CV-6 which were used for our experiments is one of these human cardiovascular (aberration: CV) isolates collected from a human coronary artery (65).

It has been studied how primarily infected *C. pneumoniae* in the respiratory tract could be translocated to arteries far away from the origin of infection. It has been discussed that *C. pneumoniae* likely infects monocytes in the lung leading to systemic dissemination (69,70). Hence, *C. pneumoniae* can migrate to the intima of blood vessels. Due to the unique developmental life cycle of *C. pneumoniae*, they can furthermore infect neighboring cells such as macrophages, vesicular smooth muscle cells and endothelial cells leading to inflammatory response reactions. Thereby, the development of atherosclerosis is promoted (42,71).

The genesis of atherosclerotic plaques in artery is caused by chronic stress stimuli such as hypertension but also by inflammation, leading to the dysfunction of the endothelium and the increased storage of low-density lipoproteins (LDL) within the intima. The oxidation of LDL (oxLDL) again causes an inflammatory response. Due to the inflammation, endothelial cells release cytokines and growth factors, resulting in recruitment of monocytes. Monocytes express adhesion molecules and interact with the endothelial cell receptor. They can further migrate into the intima and differentiate into macrophages (42). The macrophages take up oxLDL and differentiate

into foam cells that release cytokines leading to increased monocyte recruitment. The increasing inflammatory reaction within the intima promotes the development of atherosclerosis (42,71).

C. pneumoniae might promote the genesis of atherosclerotic plaques by enhancing the formation of reactive oxygen species (ROS) (72), leading to increased oxidation of LDL (73). Furthermore, *C. pneumoniae* promote the release of cytokines, which benefits inflammation process (74).

Although it is still under debate, *C. pneumoniae* might also be associated with chronic diseases such as the Alzheimer's disease (75,76), diabetes mellitus (77), Behçet's disease (78), primary biliary cirrhosis (79), lung cancer (80,81) and reactive arthritis (82,83).

Although much is known about diseases caused by *C. pneumoniae*, the lack of tools for the genetic modification of *C. pneumoniae* has hampered further molecular research that can elucidate chlamydial pathogenesis in detail.

3.2 Genetic modification of chlamydiae

3.2.1 Transformation of chlamydiae

The first transformation of chlamydiae was reported in 1994 by Tam *et al.* using electroporation to insert a plasmid called P7248::cat into the EBs of *C. trachomatis* (84). However, the chlamydial expression of P7248::cat was only transient. In 2009 Binet and Maurelli used the same technique to transfer recombinant DNA into *C. psittaci* leading to the first reported allelic exchange in chlamydiae (85). Two years later Wang *et al.* published a transformation protocol for *C. trachomatis* using a *C. trachomatis*-derived plasmid shuttle vector called pGFP::SW2 resulting in stable GFP expressing chlamydial transformants (86). Although this approach is a promising and easy-to-handle transformation protocol for chlamydiae, this method can only be applied to *C. trachomatis* due to plasmid tropism. Since Wang *et al.* published their transformation protocol using chlamydial endogenous plasmids, various different plasmid shuttle vectors for *C. trachomatis* and *C. muridarum* have been constructed (46). Nevertheless, a plasmid shuttle vector for *C. pneumoniae* is still missing. Endogenous chlamydial plasmids are crucial for the development of new plasmid shuttle vectors. Therefore, it is indispensable to have knowledge about structure and functions of plasmids.

3.2.2 Plasmids of prokaryotic cells

In addition to the chromosome, prokaryotic cells can also harbor extrachromosomal, double-strand DNA called plasmid. The plasmid can be linear or circular and can achieve a size between 1-kp till 1-Mb (87). While the chromosome encodes essential genes, plasmids contain non-essential genes that can grant special abilities to the bacterium such as resistances against antibiotics or heavy metals, virulence factors (e.g. coagulase, hemolysin or toxins) or metabolic features (e.g. metabolism of lactose, citrate, saccharose or urea) (87). These features may lead to advantages in natural selection. The plasmid's replication is independent on the chromosomal replication cycle. It is possible that a bacterium harbors several plasmid copies of the same plasmid. Copy numbers up to 100 are possible. At the same time, it is also possible that a prokaryotic cell harbors several different plasmids. During cell division the plasmids within the prokaryotic cell are randomly distributed to the new cells (87). Beside this mechanism of plasmid dissemination, it is also possible that bacteria can pick up plasmids from the environment (e.g. plasmids from dead bacteria). The more common mechanism for plasmid dissemination among bacteria is the transfer of plasmid from a donor bacterium to an acceptor bacterium using pili (conjugative pili or "sex pili"). This widespread mechanism for horizontal gene transfer is called bacterial conjugation and is a feature of special plasmids called F-plasmids (F = Fertilize) containing several genes (*tra*-region, *tra* = transfer) that are necessary for bacterial conjugation (87,88). Alongside the important role of plasmids and their dissemination during bacterial evolution, plasmids are also important tools in gene technology. For instance, artificial plasmids are used for the production of drugs such as insulin in pharmaceutical industry (89).

3.2.3 Chlamydial plasmids

Some *Chlamydia* spp. also carry extrachromosomal plasmids. Interestingly, all chlamydial plasmids are approximately 7.5-kb large and contain eight putative coding DNA sequences (CDSs) which have different functions (cf. table 2) (46,90–96). For instance, plasmid replication is supposedly regulated by CDS1 and CDS2 (96) while CDS3, CDS4 and CDS8 seem to play an key role in plasmid maintenance (96). CDS2 on the other hand also encodes antisense small RNA (sRNA-2) that appears to be associated with plasmid maintenance (97). As well as plasmid regulation and maintenance functions, CDS5 works as a virulent factor in infections of

C. trachomatis or *C. muridarum* (96). Furthermore, the glycogen synthase gene *glgA* on chlamydial chromosome is regulated by the proteins pgp4 and/or pgp5 encoded by CDS6 and CDS7 (96).

In the last decade, chlamydial plasmids became focus of new genetic modification studies. Nevertheless, transformation of chlamydiae is still challenging due to plasmid tropism.

Table 2: Coding DNA sequences (CDS) located on chlamydial plasmid and their associated function.

CDS	Function	Protein
1	Homologue of integrase	pgp7
2	Homologue of recombinase/ plasmid maintenance	pgp8
3	Homologue of DnaB helicase/ plasmid maintenance	pgp1
4	Plasmid maintenance	pgp2
5	Virulence factor/ regulation of CDS6	pgp3
6	Transcriptional activator of plasmid-dependent genes/ virulence factor/ glycogen synthesis/ regulate exit from host cells	pgp4
7	Transcriptional suppressor/ virulence factor/ regulation of plasmid-dependent genes/ plasmid replication/ glycogen synthesis	pgp5
8	Plasmid maintenance/ plasmid replication	pgp6

CDS: Coding DNA sequence; pgp: Plasmid glycoproteins
References: Comanducci *et al*. (1990); Thomas *et al*. (1997); Li *et al*. (2008); Gong *et al*. (2013); *Song et al*. (2013,2014) Sixt *et al*. (2016) and Zhong *et al.* (2017) (46,90–96).

3.2.4 Plasmid tropism

Although the transformation of *C. trachomatis* using plasmid shuttle vectors such as pGFP::SW2 (86) is quite beneficial, their use is unfortunately limited. Other *Chlamydia* spp. cannot be transformed using a shuttle plasmid vector without an endogenous chlamydial plasmid as a backbone. The challenge to cross chlamydial species barrier during chlamydial transformation was first described by Wang *et al.* (97) and Song *et al.* (95). Later Song *et al.* called this unique phenomenon “plasmid tropism” (95). According to their findings, chlamydial plasmid shuttle vectors must contain a backbone of the endogenous chlamydial plasmid. Wang *et al.* further showed that CDS2 plays a key role in plasmid tropism (97). During their experiments

they were able to transform *C. muridarium* using a *C. trachomatis*-derived plasmid shuttle vector called pGFP::SW2. Further analyses, however, show that pGFP::SW2 isolated from transformed *C. muridarum* contains the CDS2 region of *C. muridarum'*s endogenous plasmid pNigg. These findings indicated that a genetic recombination took place between the endogenous *C. muridarum* plasmid pNigg and the plasmid shuttle vector pGFP::SW2. This recombination led to the development of a new plasmid they called pSW2NiggCDS2. First the creation of the new plasmid resulted in the successful transformation of *C. muridarum* (97). The mechanisms behind plasmid tropism have not been completely deciphered to date.

3.3 Study goal

Available plasmid shuttle vectors are not suitable for *C. pneumoniae*. Hence further chlamydial research is hindered and limited. Since new plasmid shuttle vectors for *C. pneumoniae* are important tools for future investigations dealing with, for example, chlamydial pathogenesis or tissue tropism, this thesis focuses on the establishment of a transformation method for *C. pneumoniae* and the characterization of the resulting transformants.

Following challenges are conducted in this thesis:

- Development of a new *C. pneumoniae*-derived plasmid shuttle vector
- Analysis of plasmid DNA sequence of several *Chlamydia* spp.
- Transformation of different chlamydial strains to investigate the effectivity of the new constructed plasmid shuttle vector
- Investigation of the impact of the new constructed plasmid shuttle vector on chlamydial morphology
- Investigation of the impact of the new constructed plasmid shuttle vector on chlamydial growth
- Investigation of the plasmid stability in transformed *Chlamydia* spp.

4 Material

4.1 Laboratory equipment

Table 3: Laboratory equipment used in this thesis. In alphabetic order.

Item	Company
Analytical balance KB	Kern & Sohn GmbH, Balingen-Frommen, Germany
Benches	
EN 12469	Clean Air Techniek B.V., Woerden, Netherlands
Peqlab PCR workstation pro	VWR International, Radnor, Pennsylvania, United States
Centrifuges	
Universal 320 R	Hettich Zentrifugen, Tuttlingen, Germany
Rotina 38 R	Hettich Zentrifugen, Tuttlingen, Germany
Biofuge fresco	Heraeus Instruments GmbH, Hanau, Germany
Biofuge pico	Heraeus Instruments GmbH, Hanau, Germany
Biofuge 15	Heraeus Instruments GmbH, Hanau, Germany
Multifuge 3 S-R	Heraeus Instruments GmbH, Hanau, Germany
Centrifuge 5417 R	Eppendorf AG, Hamburg, Germany
Electrophoresis chambers	
Horizon 11-14	Thermo Fisher Scientific, Waltham, Massachusetts, United States
Peqlab PerfectBlue™ Gel System Mini L	VWR International, Radnor, Pennsylvania, United States
Imaging system Fusion FX7	Vilber Lourmat GmbH, Eberhardzell, Germany
Incubators (37°C, 5% CO_2)	
Forma Series II 3131	Thermo Fisher Scientific, Waltham, Massachusetts, United States
BINDER Inkubator Serie C	BINDER GmbH, Tuttlingen, Germany
Magnetic stirrer, RMO	Gerhardt GmbH, Königswinter, Germany
Microscops	
BZ-9000	Keyence, Osaka, Japan
Invitrogen EVOS FL Auto Cell Imaging System	Thermo Fisher Scientific, Waltham, Massachusetts, United States
Axiovert 25	Carl Zeiss MikroImaging, Göttingen, Germany
JEOL 1011 transmission electron microscope (TEM)	JEOL, Tokyo, Japan
NanoPhotometer® P330	Implen GmbH, München, Germany

Peltier cooler/heater PCH-2	Grants-Instruments Ltd, Shepreth, United Kingdom
Pipettes Pipette Controller accu-jet® pro Pipette Controller pipetus® Micropipette Research® (0,5-10 µL, 10-100 µL) Micropipette Reference® (0,5-10 µL, 10-100 µL, 100-1000 µL)	 Brand GmbH, Wertheim, Germany Hirschmann Laborgeräte GmbH & Co. KG, Eberstadt, Germany Eppendorf AG, Hamburg, Germany Eppendorf AG, Hamburg, Germany
Power supply units Peqlab EV231 Power Pack	 VWR International, Radnor, Pennsylvania, United States Biometra GmbH, Göttingen, Germany
Shakers and Mixers REAX 2000 REAX top VXR basic Vibrax® ThermoMixer® comfort New Brunswick™ Innova® 40/40R Shaker Universal Shaker SM 30 control	 Heidolph Instruments GmbH, Schwalbach, Germany Heidolph Instruments GmbH, Schwalbach, Germany IKA Werke GmbH, Staufen, Germany Eppendorf AG, Hamburg, Germany Eppendorf AG, Hamburg, Germany Edmund Bühler GmbH, Hechingen, Germany
Thermal cycler C1000	Bio-Rad Laboratories GmbH, Munich, Germany

4.2 Consumables

4.2.1 Consumption items

Table 4: Consumption items used in this thesis. In alphabetic order.

Item	Company
6-, 24-well cell culture plate	Greiner Bio-One GmbH, Frickenhausen, Germany
Cellstar cell culture flask 250 mL, 550 mL	Greiner Bio-One GmbH, Frickenhausen, Germany
Counting chamber BLAUBRAND® Neubauer improved	BRAND GmbH + CO KG, Wertheim, Germany
Coverslip, Ø 10 mm	Menzel-Gläser, Braunschweig, Germany
Glass beads	Karl Hecht GmbH & Co KG, Sondheim, Germany
Microscope slide (76 x 26 mm)	Menzel-Gläser, Braunschweig, Germany
Parafilm M®	Bemis, Neenah, Wisconsin, United States

Pipettes	
Biosphere® filter tip 20,100, 1000	Sarstedt AG & Co, Nümbrecht, Germany
Filter tip PP neutral (0.5-10 µL, 0-100 µL, 100-1000 µL)	nerbe plus GmbH, Winsen/Luhe, Germany
Transfer pipette 3.5 mL	Sarstedt AG & Co, Nümbrecht, Germany
Pipette 5 mL, 10 mL, 25 mL	Greiner Bio-One GmbH, Frickenhausen, Germany
Petri dish with cams	Sarstedt AG & Co, Nümbrecht, Germany
Thermanox coverslips (plastic)	Nunc Brand Products, Rochester, New York, United States
Tubes	
Safe seal micro tube 0.5-2 mL	Sarstedt AG & Co, Nümbrecht, Germany
Saphire PCR tube with attached cap 0.2 mL	Greiner Bio-One GmbH, Frickenhausen, Germany
Nalgene cryoware cryogenic vials	Thermo Fisher Scientific, Waltham, Massachusetts, United States
Tube 12 mL + cap YLW	Sarstedt AG & Co, Nümbrecht, Germany
Tube 50 mL PP	Sarstedt AG & Co, Nümbrecht, Germany

4.2.2 Chemicals and reagents

Table 5: Chemicals and reagents used in this thesis. In alphabetic order.

Item	Company
Agarose	Sigma-Aldrich Corporation, St. Louis, Missouri, United States
Araldite	Fluka, Buchs, Switzerland
Bacto™ tryptone	Thermo Fisher Scientific, Waltham, Massachusetts, United States
Bacto™ yeast extract	Thermo Fisher Scientific, Waltham, Massachusetts, United States
Calcium chloride ($CaCl_2$)	Sigma-Aldrich Corporation, St. Louis, Missouri, United States
Chloramphenicol	Sigma-Aldrich Corporation, St. Louis, Missouri, United States
Cycloheximide	Sigma-Aldrich Corporation, St. Louis, Missouri, United States
Distilled water (Aqua destillata)	Sigma-Aldrich Corporation, St. Louis, Missouri, United States
DMEM - Dulbecco's Modified Eagle Medium	Thermo Fisher Scientific, Waltham, Massachusetts, United States
Ethanol, absolute	Merck KGaA, Darmstadt, Germany
Fetal bovine serum (FBS)	Thermo Fisher Scientific, Waltham, Massachusetts, United States

GeneRuler 100 bp Plus DNA Ladder	Thermo Fisher Scientific, Waltham, Massachusetts, United States
Glucose	Sigma-Aldrich Corporation, St. Louis, Missouri, United States
Glycerol	Merck KGaA, Darmstadt, Germany
HEPES Buffer Solution	Greiner Bio-One, Frickenhausen, Germany
Isopropanol 70%	Sigma-Aldrich GmbH, Steinheim, Germany
Magnesium chloride ($MgCl_2$)	Sigma-Aldrich Corporation, St. Louis, Missouri, United States
Methanol	Merck KGaA, Darmstadt, Germany
Monopotassium phosphate (KH_2PO_4)	Merck KGaA, Darmstadt, Germany
Monosodium phosphate-Monohydrate (NaH_2PO_4 x H_2O)	Merck KGaA, Darmstadt, Germany
Mounting Fluid	Thermo Fisher Scientific, Waltham, Massachusetts, United States
PCR Nucleotide Mix (dNTP)	Roche Diagnostics GmbH, Mannheim, Germany
Potassium chloride (KCl)	Merck KGaA, Darmstadt, Germany
RedSafe™	Intron, Burlington, MA, USA
Sodium azide (NaN_3)	Merck KGaA, Darmstadt, Germany
Sodium chloride (NaCl)	Merck KGaA, Darmstadt, Germany
Sodium pyruvate	Pan-Biotech GmbH, Aidenbach, Germany
Tris	Sigma-Aldrich Corporation, St. Louis, MO, USA
Trypan blue (0.4%)	Sigma-Aldrich Corporation, St. Louis, MO, USA
Trypsin-EDTA (1x)	PAA Laboratories GmbH, Cölbe, Germany
λ DNA-HindIII DNA Ladder	Thermo Fisher Scientific, Waltham, Massachusetts, United States

4.2.3 Buffer solutions and other solutions

Table 6: Buffer solutions and other solutions used in this thesis. In alphabetic order.

Solution	Ingredients
$CaCl_2$ (Calcium chloride) buffer	10 mM Tris, 50 mM $CaCl_2$, pH 7.4
Montis Fixanz	156 mL Sodium-Cacodylate-Buffer (0,1 M), 25 mL Glutaraldehyde (25%), 19 mL Paraformaldehyde (10%), 3 mL $CaCl_2$-solution (3%), pH 3.75
Phosphate-buffered saline (PBS)	80 g NaCl, 2 g KCl, 11.5 g Na_2HPO_4 12 x H_2O, 2 g KH_2PO_4, ad 1 L A. dest., pH 7.2

Sodium-Cacodylate-Buffer (0.2 M)	42.8 g sodium cacodylate, 68.46 g Sucrose, ad 1 L A. dest.
SPG buffer	75 g Sucrose, 2.47 g Na_2HPO_4, 0.36 g NaH_2PO_4, 0.72 g L- Glutamic acid, ad 1 L A. dest., pH 7.3
TAE (TRIS-Acetate-EDTA-Puffer) buffer	40 mM Tris, 20 mM acetic acid, 1 mM EDTA
TE buffer	10 mM Tris-HCl, 1 mM EDTA, pH 8.0

4.2.4 Enzymes and kits

Table 7: Enzymes and commercial kits used in this thesis. In alphabetic order.

Item	Company
2.5 U Taq Polymerase	Invitrogen, Karlsruhe, Germany
IMAGEN Chlamydia Kit	Oxoid, Cambridgeshire, UK
NdeI (Restriction Endonucleases)	New England Biolabs, Ipswich, MA, USA
NucleoSpin Tissue Kit	Macherey-Nagel, Dueren, Germany
Qiagen Plasmid Mega Kit	Qiagen, Hilden, Germany
SalI (Restriction Endonucleases)	New England Biolabs, Ipswich, MA, USA

4.3 Culture medium

Table 8: Culture medium used in this thesis for cultivating cells and bacteria.

Culture medium	Ingredients
Cell culture medium	Dulbecco's modified Eagle medium (DMEM) supplemented with 10% fetal bovine serum (FBS), 1 mM sodium pyruvate and 30 mM HEPES
Lysogeny broth (LB) medium (liquid)	5.0 g Bacto tryptone, 2.5 g Bacto yeast extract, 5.0 g NaCl and 500 mL a. dest.
50 µg/mL CAM LB medium (solid)	5.0 g Bacto tryptone, 2.5 g Bacto yeast extract, 5.0 g NaCl, 7.5 g agar, 500 mL a. dest. and 500 µL of 50 mg/mL chloramphenicol (added after autoclavation)
SOC medium	10 g Bacto tryptone, 2.5 g Bacto yeast extract, 0.25 g NaCl, 500 mL A. dest., 5 mL of 250 mM KCl, 2.5 mL of 2M $MgCl_2$ and 10 mL of 1M glucose
BD Columbia Agar with 5% Sheep Blood (Becton Dickinson GmbH, Heidelberg, Germany)	12.0 g pancreatic digest of Casein, 5.0 g peptic digest of animal tissue, 3.0 g yeast extract, 3.0 g beef extract, 1.0 g corn starch, 5.0 g sodium chloride, 13.5 g agar, 5% sheep blood (defibrinated), pH 7.3 ± 0.2

4.4 Cell lines

Table 9: Cell lines used in this thesis.

Cell line	Collection No.	Species	Cell type	Company
Human epithelial type 2 (HEp-2) (HeLa derivative)	ATCC CCL 23	Human	Epithelial	ATCC, Manassas, Virginia, USA

4.5 Bacterial strains

Table 10: Bacterial strains used in this thesis.

Species	Strain	Origin
Chlamydia pneumonia	LPCoLN	University of Sunshine Coast, Maroochydore, Australia
	CV-6	University of Lübeck, Lübeck, Germany
Chlamydia felis	Not identified (N.I.)	University of Southampton, Southampton, United Kingdom
	Cello	University of Southampton, Southampton, United Kingdom
	02DC26 (Cf02-23)	Friedrich-Loeffler-Institut, Jena, Germany
Chlamydia trachomatis	L2 (25667R)	University of California, Irvine, CA, USA
Chlamydia muridarum	MoPn/Nigg (DSM-28544)	Friedrich-Loeffler-Institut, Jena, Germany
Chlamydia pecorum	14DC102 (E58) (DSM-29919)	Friedrich-Loeffler-Institut, Jena, Germany
Chlamydia abortus	C18/98 (B577) (DSM-27654)	Friedrich-Loeffler-Institut, Jena, Germany
Chlamydia caviae	03DC25 (GPIC) (DSM-19441)	Friedrich-Loeffler-Institut, Jena, Germany
Escherichia coli	JM110	Agilent Technologies, Santa Clara, CA, USA
	DH5α	Agilent Technologies, Santa Clara, CA, USA

4.6 Chlamydial plasmids

Table 11: Plasmid DNA sequences used for analyses in this thesis.

Plasmid	Strain	Reference
pCpnEI	*C. pneumoniae* N16	GenBank: X82078.1
LPCoLN plasmid	*C. pneumoniae* LPCoLN	GenBank: CP001714.1
pCfe1	*C. felis* Fe/C-56	GenBank: AP006862.1
CpecL1	*C. pecorum* L1	GenBank: CM003639.1
pCpGP1	*C. caviae* GPIC	GenBank: AE015926.1
pNigg	*C. muridarum* MoPn/Nigg	GenBank: AE002162.1
pL2	*C. trachomatis* L2	GenBank: AM886278.1

4.7 Plasmid shuttle vector

Table 12: Plasmid shuttle vectors used in this thesis.

Plasmid	Backbone	Size
pRSGFPCAT-Cpn	*C. pneumoniae* N16	10,038 bp
pGFP::SW2	*C. trachomatis* SW2	11,539 bp

4.8 Antibodies

4.8.1 Primary antibodies

Table 13: Primary antibodies for immunofluorescence staining used in this thesis.

Name	Origin	Manufacturer	Dilution	Specificity
Chlamydial-LPS antibodies	Mouse	Prof. H. Brade, FZ Borstel, Germany	1:50	Polyclonal

4.8.2 Secondary antibodies

Table 14: Secondary antibodies for immunofluorescence staining used in this thesis.

Name	Origin	Manufacturer	Dilution	Specificity
Anti-mouse antibodies (FITC-labeled)	Rabbit	Dako Deutschland GmbH, Hamburg, Germany	1:250	Polyclonal

4.9 Primer

Table 15: Primer used in this thesis (98–102)**.**

Primer	Sequence (5´- 3´)	Target	Length
N16 pgp F	ATGGGATCTCAGCAGATTGT	*C. pneumoniae* plasmid	20 bp
N16 pgp R	GGCTGTTGCTTGATTGATTA		20 bp
pCF01F	GGCAACTTTATCTCCAATCACC	*C. felis* plasmid	22 bp
pCF01R	CTTTCCAGCTTCATAGAACCATC		23 bp
pCFelis-F	CACACTAGGGAGACAATTTCCA	*C. felis* plasmid	22 bp
pCFelis-R	GACCACTATCCCTGAGATCCGA		22 bp
C.peco-P-F	GTTCACACTCTGCCTCATC	*C. pecorum* plasmid	19 bp
C.peco-P-R	CCTATTTATTGGCGTCTAGG		20 bp
Ct pgp-F	TCAAGGACCAGCAAATAATC	*C. trachomatis* plasmid	20 bp
Ct pgp-R	GAATAACCCGTTGCATTGAA		20 bp
C.cavi-P-F	CAGGTCTTGCAGCGACAACA	*C. caviae* plasmid	20 bp
C.cavi-P-R	ACGTTCACCGTTCACGCTTA		20 bp
C.muri-P-F	TGTCACAGCGGTTGCTCTAA	*C. muridarum* plasmid	20 bp
C.muri-P-R	CTATGCTGCAAGGAGGTAAG		20 bp

4.10 Software

Table 16: Computer software used in this thesis. In alphabetic order.

Software	Company
Adobe Photoshop CS2	Adobe Systems Inc., San Jose, CA, USA
BLAST: Basic Local Alignment Search Tool	National Institutes of Health, Bethesda, MD, USA
BZ Analyzer Software	Keyence, Osaka, Japan
DeepL Translator	DeepL GmbH, Cologne, Germany
Fusion	Vilber Lourmat Deutschland GmbH, Eberhardzell, Germany
GraphPad Prism	GraphPad Software Inc., La Jolla, CA, USA
Image J	National Institutes of Health, Bethesda, MD, USA
LEO (Machine-readable dictionary)	LEO GmbH, Sauerlach, Germany
Microsoft Office	Microsoft, Redmond, Washington, USA
Mozilla Firefox	Mozilla Foundation, Mountain View, CA, USA
Snap Gen	GSL Biotech LLC, Chicago, IL, USA
Zotero	Center for History and New Media at George Mason University, Fairfax, Virginia, USA

5 Methods

5.1 Culture

All working steps were performed using clean benches to avoid contamination.

5.1.1 Bacterial culture

Escherichia coli (*E. coli*) was cultivated using SOC medium, BD Columbia Agar with 5% Sheep Blood or LB medium (liquid or solid). Depending on the requirements of the experiment, different incubations conditions were used.

5.1.1.1 Medium

Ingredients of different mediums (cf. table 8) were mixed in a suitable reaction vessel and dissolved in a. dest. followed by autoclavation. Afterwards the medium was aliquoted to plates, vessels, or tubes and stored. When antibiotics such as chloramphenicol (CAM) were needed, they were added to medium after autoclavation and after the medium was cooled down (around 50°C).

In the case of SOC medium, KCl, $MgCl_2$ and glucose were also first added after autoclavation and after the medium was cooled down (around 50°C).

BD Columbia Agar with 5% Sheep Blood was commercially obtained from Becton Dickinson GmbH, Heidelberg, Germany.

5.1.2 Cell culture

HEp-2 cells were used as host cells and to maintain a successful cultivation of chlamydiae. The HEp-2 stocks used in our laboratory were frequently checked by PCR to avoid contamination with *Mycoplasma.*

5.1.2.1 HEp-2 cell culture

HEp-2 cell cultures were cultured in a cell culture flask filled with 25 mL of cell culture medium and cultivated in an incubator with 5% CO_2 at 37°C. Afterwards, HEp-2 cells were harvested, counted, and seeded into 6- or 24-well cell culture plates for further experiments. For harvesting the HEp-2 cells, the used 25 mL cell culture medium was discarded, and HEp-2 cell monolayer within the cell culture flask was washed with PBS. Trypsin-EDTA was added to the HEp-2 cells and were incubated for 5 min in an incubator to detach HEp-2 cells from the cell culture flask. Afterwards

the Trypsin-EDTA activity was inhibited adding 6 mL of the cell culture medium. Finally, cell suspension was counted to determine cell concentration and new cell culture plates were filled with the required cell concentration.

5.1.2.2 Cell counting

A total of 10 µL cell suspension was mixed with 80 µL PBS and 10 µL trypan blue, resulting in a stained 1:10 cell dilution (dilution factor). Afterwards, 10 µL of the cell dilution was filled into a hemocytometer, which was used to count HEp-2 cells on an area of 1 mm^2 under a microscope (10x magnification). To calculate the concentration of the original cell suspension, the dilution factor and the counted cell number were substituted into following equation:

$$cells/mL = \frac{counted\ cell\ number\ x\ dilution\ factor\ x\ 10^4}{4}$$

5.2 Bacterial stocks

All working steps were performed using clean benches to avoid contamination.

5.2.1 Stock preparation of chemical competent *E. coli*

To improve transformation outcome for *E. coli,* chemical competent *E. coli* stocks were prepared. *E. coli* was cultured overnight in 10 mL liquid LB medium at 37°C and continuously shaking. The next day 3 mL of the culture was added to 300 mL fresh LB medium and was cultured at 37°C and continuously shaking for several hours until the optical density (OD) of 0.5 was achieved. The OD was monitored with a photometer (NanoPhotometer® P330) using 590 nm. When the final OD was reached, the 300 mL LB medium was spread into six different 50 mL conical tubes (cold). They were stored for 10 min on ice to cool down the medium. Afterwards, the tubes were centrifuged at 1000 x *g* for 15 min at 4°C to form a cell pellet at the bottom of the tubes. After the supernatant was discarded, the tubes were filled with 10 mL cold $CaCl_2$ buffer (50 mM) and centrifuged at 400 x g for 3 min at 4°C again. This step was repeated and after discarding the supernatant, 2 mL cold $CaCl_2$/glycerol solution (50 mM $CaCl_2$ and 15% glycerol) was added to the pellet. After at least 2 h of incubation on ice, 1.5 mL tubes were filled each with 200 µL of the *E. coli* suspension and immediately frozen with liquid nitrogen (LN_2) and stored first at

-25°C and finally at -80°C. The generated *E. coli* stocks were screened for contamination. For this purpose, a BD Columbia Agar with 5% Sheep Blood was incubated with a representative new generated *E. coli* stock sample and cultivated overnight at 37°C.

5.2.2 Stock preparation of *Chlamydia* spp.

5.2.2.1 Stock preparation

For stock preparation five 6-well plates with 1 x 10^6 HEp-2 cells per well were infected with chlamydiae. After 72 h incubation with 5% CO_2 at 37°C, the infected HEp-2 cells were scraped, and the cells were collected in 50 mL tubes and lysed for 5 min with glass beads (sterile). After cell lyses, the suspension was centrifuged at 200 x *g* for 5 min at 5°C. After primary centrifugation, the supernatant was centrifuged at 13000 x *g* for 90 min at 4°C to form a chlamydiae pellet at the bottom of the tube. That pellet was resolved in 1.5 mL SPG buffer, allotted to 1.5 mL tubes (20 µL per tube) and stored on ice before freezing them at -80°C. The inclusion-forming-unit (IFU) was determined to evaluate the infectiousness. The generated chlamydiae stocks were screened for contamination. Therefore, a BD Columbia Agar with 5% Sheep Blood was incubated with a representative chlamydiae stock sample and cultivated overnight at 37°C to exclude bacterial contamination. In addition, PCR was performed as well to exclude *Mycoplasma* contamination.

5.2.2.2 Determination of inclusion-forming-unit (IFU)

The infectiousness of chlamydiae was represented by the IFU. To determinate the IFUs, a 24-well plate with HEp-2 cell monolayer supplemented with 1 µg/mL cycloheximide were infected with chlamydiae. The first well was infected with 4 or 8 µL of a chlamydial stock (diluted 1:50 or 1:500) and diluted again into the next following well (1:5) (cf. figure 3). Afterwards the infected well plate was centrifuged at 700 x *g* for 1 h at 35°C followed by incubation.

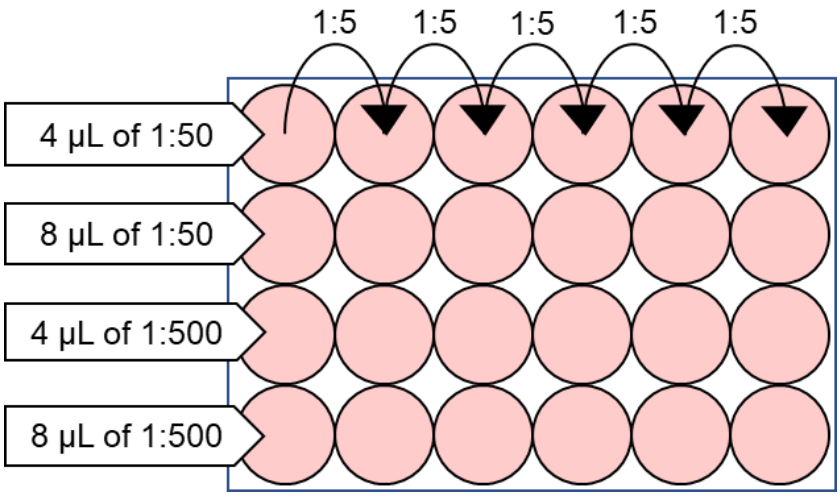

Figure 3: Determination of the IFU.
24-well-plate with HEp-2 cell monolayer (pink) was infected with 4 or 8 µL of chlamydial stock (diluted 1:50 or 1:500) and diluted into the next following well (1:5).

After 48 h incubation with 5% CO_2 at 37°C, the culture medium was discarded and the remaining HEp-2 cells including the chlamydial inclusion at the bottom of each well (200 mm^2) were fixated with methanol (15 min, -20°C) followed by staining using immunofluorescence antibodies. After staining, the chlamydial IFUs were counted under the microscope using 40x magnification for *C. pneumoniae* (field of view = 0,139 mm^2) and 20x magnification for *C. felis* (field of view = 0,557 mm^2). For the final determination of chlamydial infectiousness, the IFUs of 10 field of views were counted and added to following equation:

$$IFU\ quantity = \frac{counted\ IFUs\ x\ 200\ mm^2}{10\ x\ added\ volume\ to\ the\ well\ [\mu L]\ x\ field\ of\ view\ \ [mm^2]}$$

5.3 Staining

5.3.1 Staining of HEp-2 cells

5.3.1.1 Cell counting

For cell counting, HEp-2 cells were stained with trypan blue. Living cells were counted using a microscope (e.g. Zeiss Axiovert 25).

5.3.1.2 Counterstain

Infected HEp-2 cells were stained with the IMAGEN Chlamydia Kit. After staining, HEp-2 cells are shown in red (evans blue) using a fluorescence microscope. Counterstain was used during chlamydial direct immunofluorescence staining.

5.3.2 Staining of *Chlamydia* spp.

5.3.2.1 Direct immunofluorescence staining

Direct immunofluorescence staining was used for morphological analyses of chlamydial inclusions.

For direct immunofluorescence staining, coverslips with infected cells were fixated in 24-well plates with 1 mL methanol for 15 min at -20°C. Afterwards, the coverslips were dried at room temperature. The dry coverslips were stained with 10 µL of IMAGEN Chlamydia Kit's solution followed by an incubation for 20 min at 37°C. After incubation, the stained coverslips were washed twice with PBS and fixated with the Mounting Fluid (component of IMAGEN Chlamydia Kit) on a microscope slide. The stained samples were analyzed using a fluorescence microscope (e.g. Keyence BZ-9000). Using a fluorescence microscope, HEp-2 cells are shown in red (evans blue) and chlamydial inclusions are shown in green (FITC). Stained samples were stored at 4°C.

5.3.2.2 Indirect immunofluorescence staining

Indirect immunofluorescence staining was used for counting chlamydial IFUs under the fluorescence microscope.

For indirect immunofluorescence staining, infected cells in 24-well-plate were fixated with 1 mL methanol for 15 min at -20°C. Before fixating, the medium was discarded. Afterwards the methanol was discarded and 300 µL of a chlamydial-LPS antibody (primary antibody; cf. table 13) were added to each well of the 24-well-plate and incubated in darkness for 45 min at 37°C. After the 24-well-plate was washed twice with PBS, wells were filled with 300 µL of an FITC-labeled anti-mouse antibody (secondary antibody; cf. table 14) and incubated again in darkness for 45 min at 37°C. After washing with PBS twice, the stained samples were analyzed using a fluorescence microscope (e.g. Keyence BZ-9000). The stained chlamydial inclusions are shown in green (FITC). The stained samples were stored at 4°C.

5.4 Microscopy

5.4.1 Bright-field microscopy

Bright-field microscopy was used to observe the morphology of HEp-2 during cultivation or counting (additional staining was needed). For this purpose, the Zeiss Axiovert 25 was used.

5.4.2 Fluorescence microscopy

All fluorescence images shown in this thesis were taken with the fluorescence microscope Keyence BZ-9000 according to the manufacturer's instructions. The fluorescence signal of the red-shifted green fluorescent protein gene (RSGFP), which was expressed by pRSGFPCAT-Cpn bearing *Chlamydia* spp., could be detected as green signals within the chlamydial inclusions without immuno-staining. Furthermore, untransformed *Chlamydia* spp. were stained with antibodies to enhance visibility of chlamydial inclusions under the microscope. Chlamydial inclusions could be detected as green fluorescence signals (FITC).

HEp-2 cells were stained as previously described and could be detected as a red fluorescence signal which was used as counterstain (evans blue).

In addition, phase contrast images were also taken by Keyence BZ-9000.

5.4.3 Transmission electron microscopy (TEM)

Infected host cells were cultured on Thermanox coverslips placed in 24-well plates and incubated for 24 h, 48 h and 72 h at 37°C and 5% CO_2. After incubation, the culture medium was discarded, and the Thermanox coverslips were fixed with Montis Fixanz (cf. table 6). The fixation was performed for 1 h at RT and in darkness. Afterwards post fixation was performed with 1% OsO_4 in 0.1 M cacodylate buffer for 2 h. After post fixation, the samples were dehydrated by using graded ethanol series and were then embedded in Araldite. For the final TEM analyses, ultrathin sample pieces were stained with uranyl acetate and lead citrate and were observed with a JEOL 1011 transmission electron microscope (TEM).

The post fixation, the dehydration steps, the embedding in Araldite and the TEM images were kindly performed by the research group of Prof. Matthias Klinger in the Institute of Anatomy of the University of Lübeck (Lübeck, Germany).

5.5 *Polymerase chain reaction (PCR)*

5.5.1 PCR

The PCR sample was mixed with TE buffer and was boiled for 10 minutes. Afterwards 5 µL of the boiled sample was added as a PCR template to the PCR reaction mixture (in total 50 µL), including 10x PCR buffer (delivered with polymerase; 5µL), 20 mM deoxyribonucleoside triphosphate (dNTP) mix (0.5 µL), 50 mM $MgCl_2$ (1.5 µL), 20 µM primer (reverse and forward; each 1.25 µL), 2.5 U Taq polymerase (0.25 µL) and A. dest. (35.25 µL). Depending on the primer (cf. table 15) different PCR protocols were used (cf. table 17).

5.5.2 PCR protocols

At least 30 cycles were performed for every PCR run to guarantee complete amplification of the target gene region.

Table 17: **PCR protocols used in this thesis.**

Primer	First denaturing	Denaturing	Annealing	Extension	Final delay
N16 pgp F	94°C for 5 min	94°C for 30 sec	47°C for 1 min	72°C for 1 min	72°C for 7 min
N16 pgp R					
pCF01F	95°C for 5 min	95°C for 30 sec	54°C for 1 min	72°C for 1 min	72°C for 7 min
pCF01R					
pCFelis-F	95°C for 5 min	95°C for 30 sec	54°C for 1 min	72°C for 1 min	72°C for 7 min
pCFelis-R					
C.peco-P-F	95°C for 5 min	95°C for 30 sec	47°C for 1 min	72°C for 1 min	72°C for 7 min
C.peco-P-R					
Ct pgp-F	94°C for 5 min	94°C for 30 sec	47°C for 1 min	72°C for 1 min	72°C for 7 min
Ct pgp-R					
C.cavi-P-F	95°C for 5 min	95°C for 30 sec	47°C for 1 min	72°C for 1 min	72°C for 7 min
C.cavi-P-R					
C.muri-P-F	95°C for 5 min	95°C for 30 sec	47°C for 1 min	72°C for 1 min	72°C for 7 min
C.muri-P-R					

5.5.3 Gel electrophoresis

To investigate the results of PCR, gel electrophoresis was performed. A DNA ladder (e.g. GeneRuler 100 bp Plus DNA Ladder; 10 µL), a positive control (10 µL), a negative control (A. dest.; 10 µL) and 10 µL of the PCR product were applied to a 3% agarose gel including the nucleic acid staining solution RedSafe™. Before loading, the samples were mixed with 2 µL loading buffer. Electrophoresis

was performed for 1 h with 121V. Afterwards the gel was analyzed with the imaging system Fusion FX7.

5.6 pRSGFPCAT-Cpn shuttle vector

5.6.1 Construction

The plasmid shuttle vector pRSGFPCAT-Cpn (10,038 bp) was constructed using the 2,670 bp fragment of VspI-cleaved pRSGFPCAT vector and the 7,368 bp fragment of NdeI-cleaved plasmid pCpnE1 from *C. pneumoniae* N16 (GenBank accession no. X82078.1). Besides the chlamydial backbone from pCpnE1 (including 8 CDSs), the novel pRSGFPCAT-Cpn contains the pUC ori, the meningococcal class I protein promoter (MCIP) derived from *Neisseria meningitidis* MC50, the red-shifted green fluorescent protein gene (RSGFP) and the chloramphenicol acetyltransferase gene (CAT), which was fused to the RSGFP gene.

The construction of the plasmid shuttle vector (pRSGFPCAT-Cpn) was kindly performed by the research group of Prof. Ian Clarke in the University of Southampton (Southampton, United Kingdom).

5.6.2 Verification

The constructed plasmid shuttle vector was confirmed by following overnight digestion of pRSGFPCAT-Cpn with the restriction endonucleases SalI and NdeI.

After digestion, gel electrophoresis was performed. Two DNA ladders (GeneRuler 100 bp Plus DNA Ladder and λ DNA-HindIII digest respectively 10 µL), positive controls (each 10 µL), negative controls (each 10µL) and digested samples (each 10 µL) were applied to a 1% agarose gel including the nucleic acid staining solution RedSafe™. Before loading, the samples were mixed with 2 µL loading buffer. Electrophoresis was performed with 121V for 1 h. Afterwards the gel was analyzed with the imaging system Fusion FX7.

Furthermore, DNA sequencing of pRSGFPCAT-Cpn was also performed. Plasmid DNA sequencing was kindly performed by Prof. Ian Clarke in the University of Southampton (Southampton, United Kingdom). Plasmid maps were generated and visualized with the computer software SnapGene. CLUSTLW (GenomeNet) was used to analyze sequence results.

5.7 Genetic transformation

All working steps were performed using clean benches to avoid contamination.

5.7.1 Transformation of *E. coli*

A total of 200 µL chemical competent *E. coli* were incubated with ca. 25 µg plasmid for 30 min on ice. Afterwards the sample was heated at 42°C for 30 seconds followed by 3 min incubation on ice. After adding 800 µL SOC solution, the suspension was incubated for 1 h at 37°C and continuous shaking. Finally, the *E. coli* suspension was spread to 50 µg/mL CAM LB medium plates (solid) and incubated with 5% CO_2 at 37°C. Growing *E. coli* colonies were further cultured in liquid LB medium supplemented with CAM (50 µg/mL) and used for plasmid isolation.

5.7.2 Transformation of *Chlamydia* spp.

Successful transformation was evaluated after passage 5 or at least after 40 days of incubation.

5.7.2.1 Transformation

Genetic transformation of *Chlamydia* spp. was performed using modified transformation protocols, described in previous studies (86). For transformation, 6-15 µg of the plasmid shuttle vector was mixed with 1 x10^7-IFU of *Chlamydia* spp. and incubated with 200 µL of $CaCl_2$ buffer for 30 min at room temperature. In parallel previous harvested and counted (4 x 10^6) HEp-2 cells were also incubated with 200 µL of $CaCl_2$ buffer for 30 min at room temperature. Afterwards they were added to the 200 µL chlamydiae suspension (in total 400 µL) and incubated again for further 20 min at room temperature. The previously described incubation steps were performed by continuously and moderate shaking. After incubation was completed, four wells (two with coverslips) of a 6-well plate were filled each with 2 mL of cell culture medium (supplemented with 1 µg/mL cycloheximide) and 100 µL of the Chlamydiae-pRSGFPCAT-Cpn-HEp-2-cell suspension. The mixture was centrifugated at 700 x *g* for 1 h at 35°C. After centrifugation, the 6-well plate was incubated with 5% CO_2 for 72 h at 37°C. After incubation, new subculture was prepared. In addition, chlamydial infection rate was checked by stained coverslips (IMAGEN Chlamydia Kit).

5.7.2.2 Subculture

Subcultures were performed after 48 or 72 h.p.i. to evaluate transformation and expression of RSGFP.

Infected HEp-2 cell monolayer (from previous culture) was scraped and lysed by glass beads (sterile) for 5 min. Afterwards, the sample was centrifuged at 200 x *g* for 5 min at 4°C to separate cell debris and chlamydiae. A total of 2 mL of supernatant was added to 1 x 10^6 HEp-2 cell monolayer, which were prepared the day before. The medium was supplemented with CAM (concentration depends on experiment) and 1 µg/mL cycloheximide. New generated subcultures were centrifuged at 700 x *g* for 1 h at 35°C. Afterwards, they were incubated with 5% CO_2 at 37°C.

Glass coverslips were added to the wells in subculture 1 to observe chlamydial infection rate.

5.8 Recovery assay

All working steps were performed using clean benches to avoid contamination.

For the recovery assay, HEp-2 cells were prepared in 24-well plates. During cell cultivation glass coverslips for the immunofluorescence microscopy and Thermanox coverslips for TEM images were added to the 24-well plates (cf. figure 4). Afterwards, the 24-well-plates containing 0.5 x 10^5 HEp-2 cells per well were supplemented with cycloheximide (1 µg/mL) and CAM (0.8 µg/mL for *C. pneumoniae* LPCoLN and 1.1 µg/mL for *C. pneumoniae* CV-6). Cells were either infected with 2 x 10^5 IFU wild type (untransformed) or transformed *C. pneumoniae* (cf. figure 4). Subsequently, the 24-well-plates were centrifuged at 700 x *g* for 1 h at 35°C. Plates were incubated for 5 h, 24 h, 48h or 72 h at 37°C and 5% CO_2.

After incubation was completed, the glass coverslips were analyzed by an immunofluorescence microscope. In addition, the Thermanox coverslips were analyzed using TEM. The remaining wells were used for determination of the IFU.

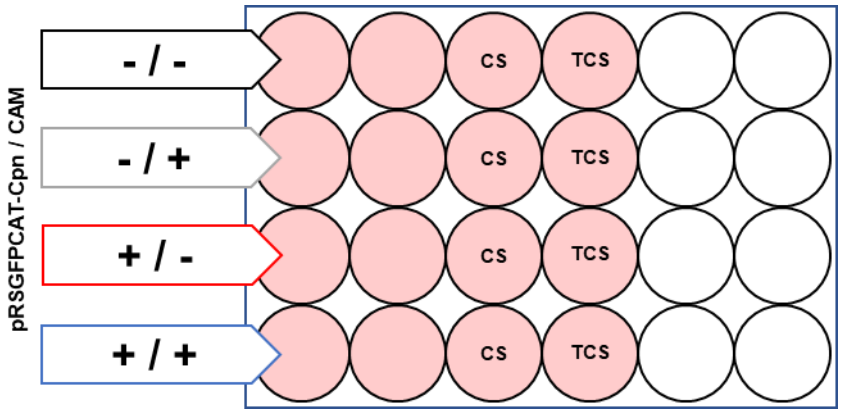

Figure 4: **Recovery assay for chlamydial growth and morphology.**
24-well-plate with 0.5 x 10^5 HEp-2 cells per well are shown in pink. During cell cultivation coverslips (CS) and Thermanox coverslips (TCS) are added to the wells. Afterwards the 24-well-plate was infected with pRSGFPCAT-Cpn transformed or wild type *C. pneumoniae* [+: transformed; -: non-transformed (= wild type)]. Medium was supplemented with CAM (+: added; -: not added).

5.9 Plasmid stability test

All working steps were performed using clean benches to avoid contamination.

To investigate plasmid stability of pRSGFPCAT-Cpn during cultivation, HEp-2 cells were infected with *C. pneumoniae* (0.5 IFU/cell) and cultivated in the presence or absence of CAM (0.8 µL/mL) as previously described. Multiple subcultures were performed as previously described and the IFU was determined respectively. RSGFP signals were used for IFU determination of transformed chlamydiae. Indirect immunofluorescence staining was used to count the total number of IFU (transformed and non-transformed chlamydiae). For this purpose, the fluorescence microscope (Keyence BZ-9000) was used to count the IFUs in 24 independent pictures (40x magnification = 1.4 mm^2). After counting, the IFU quantity was calculated using following equation:

$$IFU/mL \; x \; 10^5 = \frac{counted\ IFU\ in\ 1.4\ mm^2 x\ 2}{1.4\ x\ added\ volume\ to\ the\ well\ [\mu L]}$$

The ratio of IFU generated by RSGFP signal compared to the IFU generated by immunofluorescence signal was used to analyze plasmid stability of pRSGFPCAT-Cpn. This procedure was performed for five subcultures. New subcultures were made in an interval of two or four days.

5.10 Whole-genome sequencing

Chlamydiae were cultured as previously described. Chlamydial genome isolation was performed with NucleoSpin Tissue Kit and proteinase K digestion using the manufacturer's instruction. DNA sequencing was performed by Prof. Stefan Niemann and Dr. Thomas A. Kohl in the Department of Molecular and Experimental Mycobacteriology at the Research Center Borstel (Borstel, Germany). Sequence analyses were performed by Prof. Thomas Rattei and Dr. Javier Geijo in the University Vienna (Vienna, Austria).

5.11 Plasmid sequencing

Chlamydiae were transformed and cultured as previously described. Qiagen Plasmid Mega Kit was used for plasmid isolation following the manufacturer's instructions. Later plasmid DNA sequencing was performed by our laboratory collaborating colleagues of the University of Southampton (Southampton, United Kingdom) managed by Prof. Ian Clarke. Plasmid maps were generated and visualized with the computer software Snap Gen. CLUSTALW from GenomNet was used for further DNA sequence analyses.

5.12 Chlamydial wild type plasmid analyses

Various wild type plasmid DNA sequences of *Chlamydia* spp. were analyzed. For this purpose, we used the plasmid DNA sequences provided by the National Center for Biotechnology Information (NCBI). Analyses were performed using the Needleman-Wunsch Global Align Nucleotide Sequences algorithm of the Basic Local Alignment Search Tool (BLAST).

Three independent criteria are used for consistent classification of plasmid genes. These criteria were derived from the findings of Thomas *et al*. (91):

1. Computer-generated CDS (coding DNA sequence) from the NCBI are equal to the ORFs (open reading frame).
   "The computer-generated ORFs are numbered so that ORF 1 follows directly after the origin of replication."(91)

2. Tandem repeats
    a. “All chlamydial plasmids have four 22 bp tandem repeats in the intergenic region between ORFs 8 and 1. In plasmids from other bacterial species, tandem repeats or iterons are involved in plasmid replication, control of copy number and incompatibility”(91)
    b. “The 22 bp tandem repeats are the most highly conserved region common to all chlamydial plasmids.”(91)
3. “The computer-predicted initiation codon for each ORF is also conserved between plasmids: ATG for ORFs 1, 3, 4, 5 and 6, and GTG for ORFs 7/8.”(91)

Using these criteria, eight putative chlamydial plasmid DNA sequences were defined and classified as CDS 1-8. This classification was used for all analyses, that are shown in this thesis.

5.13 Statistical analyses

All data are shown as mean ± standard error of the mean (SEM).

The statistic program GraphPad Prism 7 was used for statistical analyses.

When one-way analysis of variance shows statistically significant value ($p \leq 0.05$), Sidak’s multiple comparison was performed. p value of $p \leq 0.05$ was considered as statistically significant. All experiments were confirmed at least in three independent experiments.

6 Results

We established an easy-to-handle transformation protocol for *C. pneumoniae* using a *C. pneumoniae*-derived plasmid shuttle vector called pRSGFPCAT-Cpn. This novel plasmid shuttle vector enables genetic transformations of animal isolate *C. pneumoniae* LPCoLN, as well as human isolate *C. pneumoniae* CV-6. In addition, we demonstrated that pRSGFPCAT-Cpn can also be used for the transformation of *C. pneumoniae* related *C. felis.* During our transformation experiments pRSGFP-CAT-Cpn had no impact on chlamydial growth or morphology. Successful transformations were achieved even without antibiotic selection pressure. The results of our investigations are shown in following chapter.

6.1 Construction of the plasmid shuttle vector pRSGFPCAT-Cpn

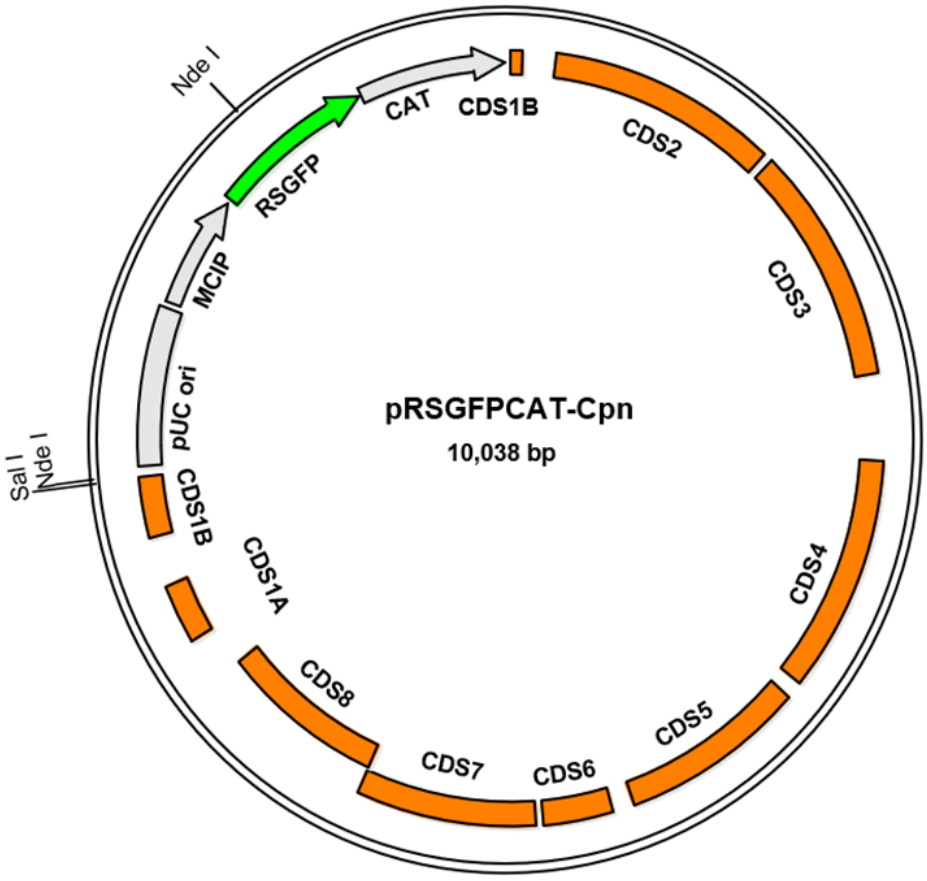

Figure 5: pRSGFPCAT-Cpn plasmid shuttle vector.
The coding DNA sequences 1-8 (CDSs) of animal isolate *C. pneumoniae* N16 plasmid pCpnE1 is shown in orange. The RSGFP gene is shown in green and the meningococcal class I protein promoter (MCIP); the chloramphenicol acetyltransferase gene (CAT) as well as the pUC ori gene are shown in light gray.

The shuttle vector was constructed using the plasmid extracted from the equine *C. pneumoniae* N16 called pCpnEI (7,368 bp; GenBank accession no. X82078.1) and the vector pRSGFPCAT. Respectively pCpnEI and pRSGFPCAT were cleaved by the restriction enzyme NdeI and VspI. Afterwards pCpnEI was ligated into the pRSGFPCAT, resulting in the 10,038 bp *C. pneumoniae*-derived plasmid shuttle vector pRSGFPCAT-Cpn (cf. figure 5). The gene of the RSGFP that is regulated by the MCIP is encoded in pRSGFPCAT-Cpn to assess the transformation of *C. pneumoniae.* In addition, the novel plasmid shuttle vector also contains the CAT gene which was used for selection of transformants. Accuracy of constructed plasmid shuttle vector was confirmed by digestion using restriction enzymes (cf. figure 6) and additional sequence analysis (cf. figure 7). A 10,038 bp fragment (cf. figure 6C) as well as a 1,476 bp and an 8,562 bp fragment (cf. figure 6D) digested by either SalI or NdeI were confirmed. DNA sequence analysis of pRSGFPCAT-Cpn validated our expected results (cf. figure 7).

Figure 6: Verification of pRSGFPCAT-Cpn shuttle vector using restriction enzymes.
pRSGFPCAT-Cpn was digested by the restriction endonuclease SalI, leading to a 10,038 bp (1) linear plasmid or by the restriction endonuclease NdeI, leading to a 1,476 bp (3) and a 8,562 bp (2) plasmid fragment.
*: 100 bp Plus DNA ladder
**: λ DNA-HindIII digest

	(A)	(B)	(C)	(D)
Sal I buffer	+	-	+	-
Nde I buffer	-	+	-	+
Sal I	-	-	+	-
Nde I	-	-	-	+

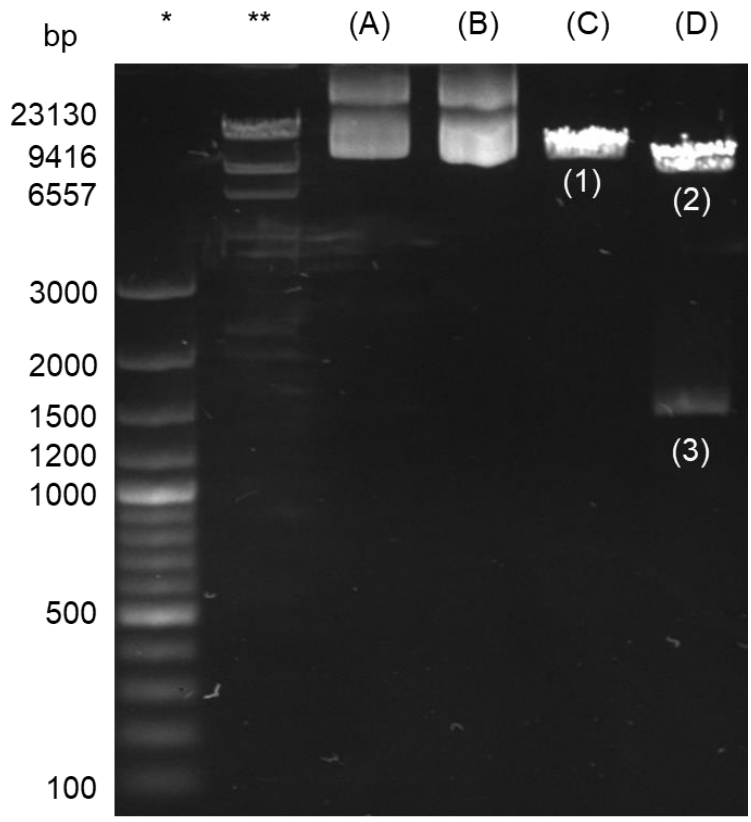

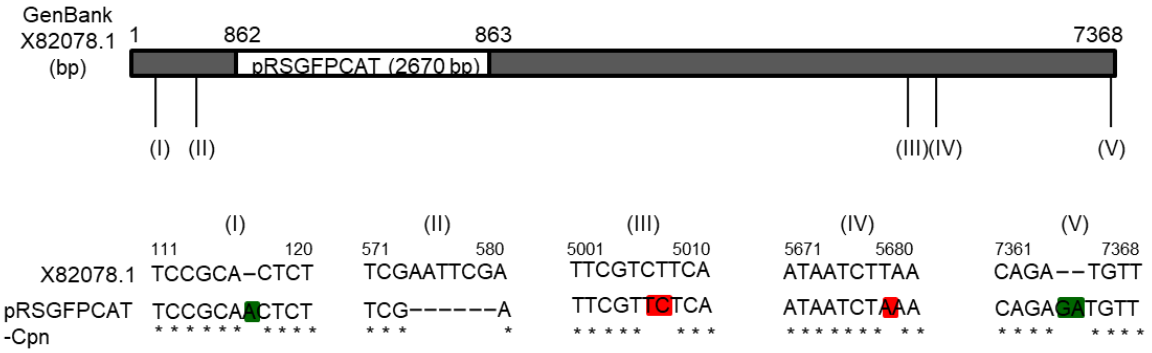

Figure 7: DNA sequence analysis of pRSGFPCAT-Cpn.
pRSGFPCAT-Cpn includes the nucleotide sequence of pCpnE1 (GenBank accession no. X82078.1) represented in gray and the nucleotide sequence of pRSGFPCAT represented in white. Sequence analyzes showing three additional (green), six deleted (AATTCG) and three changed (red) nucleotides comparing pRSGFPCAT-Cpn to the original sequence of pCpnE1 (GenBank accession no. X82078.1). The nucleotide sequence of pRSGFPCAT shows no changes.

Unfortunately, after constructing pRSGFPCAT-Cpn no *C. pneumoniae* N16 strain was available for our research. Therefore, we analyzed the plasmid DNA sequence homology between *C. pneumoniae* N16 and other *Chlamydia* spp. using the Needleman-Wunsch Global Align Nucleotide Sequences algorithm of the Basic Local Alignment Search Tool (BLAST) to look for another potential candidate for successful genetic transformation. Due to the lack of extrachromosomal plasmid, human isolated *C. pneumoniae* such as *C. pneumoniae* CV-6 was excluded from this analysis (cf. table 18). DNA analysis of total CDS in various chlamydial species showed 94% similarity between the *C. pneumoniae* N16 plasmid pCpnEI and the plasmid of *C. pneumoniae* LPCoLN called pCpnKo (cf. table 18). In the partial analysis of CDSs (CDS2 to CDS8), 98% to 99% of sequence homology was observed between pCpnEI and pCpnKo. On the other hand, CDS1 achieved only a 59% homology due to a point mutation of CDS1 that resulted in truncated CDS1A and CDS1B in pCpnEI.

Due to our analysis, we hypothesize that a high plasmid homology should correlate with a high chance of successful transformation. Therefore, we chose the available strain of *C. pneumoniae* LPCoLN for our first transformation experiments.

Table 18: Plasmid DNA sequence homology between animal isolate *C. pneumoniae* N16 and other *Chlamydia* spp.

Species	Strain	Plasmid	all CDS	CDS 1	CDS 2	CDS 3	CDS 4	CDS 5	CDS 6	CDS 7	CDS 8
C. pneumoniae	N16	pCpnEI	100	100	100	100	100	100	100	100	100
C. caviae	GPIC	pCpGP1	65	47	64	67	67	65	76	60	64
C. felis	Fe/C-56	pCfe1	65	47	67	68	77	64	76	70	62
C. muridarum	MoPn/Nigg	pMoPn	59	44	62	59	67	60	70	61	58
C. pecorum	L1	CpecL1	65	47	65	69	76	65	75	64	64
C. pneumoniae	LPCoLN	pCpnKo	94	59	99	99	99	98	99	98	99
C. trachomatis	L2	pL2	60	47	61	59	66	60	68	50	57

Homology is indicated in percent (%). *Chlamydia* spp. are arranged in alphabetic order. Human isolate *C. pneumoniae* are not analyzed due to their lack of extrachromosomal plasmids.

6.2 Genetic transformation of *C. pneumoniae* LPCoLN

Fluorescence microscope revealed a strong RSGFP signal within chlamydial inclusions in transformed *C. pneumoniae* LPCoLN at 48 h.p.i. (cf. figure 8). Since no RSGFP gene is naturally located on both the chlamydial genome and the extrachromosomal plasmid, a positive RSGFP signal is associated with successful transformation of *C. pneumoniae* using pRSGFPCAT-Cpn.

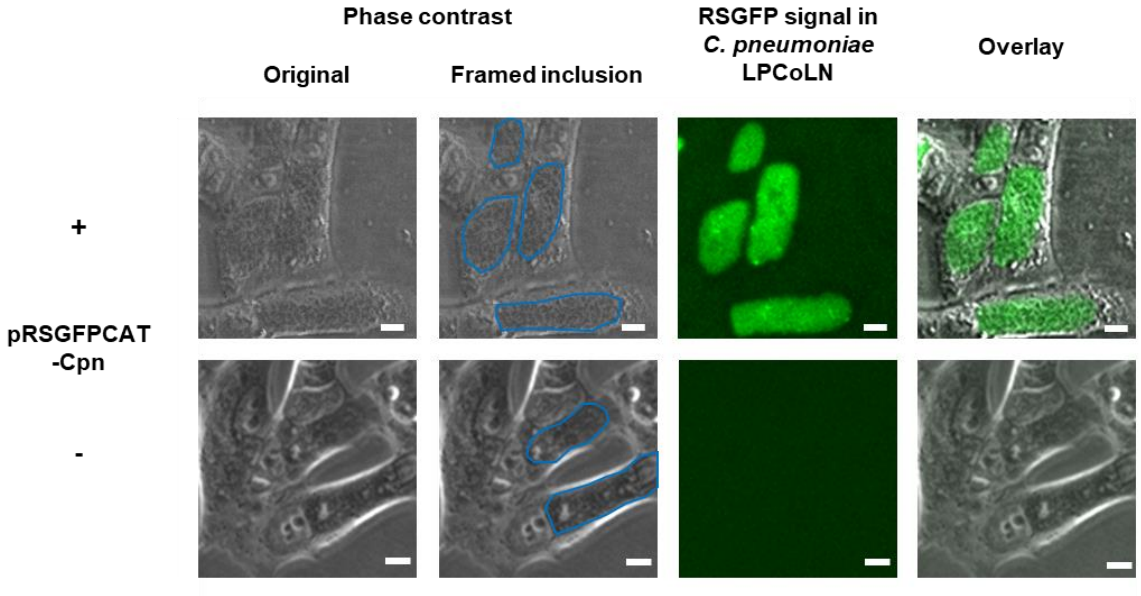

Figure 8: Representative images of successful transformed *C. pneumoniae* LPCoLN.
Successful transformation of *C. pneumoniae* LPCoLN with pRSGFPCAT-Cpn (+) compared to non-transformed *C. pneumoniae* LPCoLN (-).
The RSGFP signal (green) in chlamydial inclusions was detected after 48 h.p.i. using a fluorescence microscope. The images were taken in living host cells (HEp-2) without staining or fixing. Chlamydial inclusions were framed in blue. The scale bar represents 10 µm.

To investigate potential effects of pRSGFPCAT-Cpn on growth of transformed *C. pneumoniae* LPCoLN, recovery assays were performed in the presence and absence of CAM (cf. figure 9). When recoverable *C. pneumoniae* were analyzed at 5, 24, 48 and 72 h.p.i., no significant differences were observed between wild type and transformed *C. pneumoniae* LPCoLN without CAM treatment. Furthermore, growth pattern of transformed *C. pneumoniae* was not altered in the presence of CAM. In addition, representative fluorescence microscope and transmission electron microscope (TEM) images were taken at 24, 48 and 72 h.p.i. (cf. figure 10 and 11) to

analyze morphological characteristics. We observed similar chlamydial morphology between wild type *C. pneumoniae* and pRSGFPCAT-Cpn transformed *C. pneumoniae*. Since no IFUs were observed in previous fluorescence images of CAM treated wild type and untransformed *C. pneumoniae*, no additional TEM images were taken from this condition.

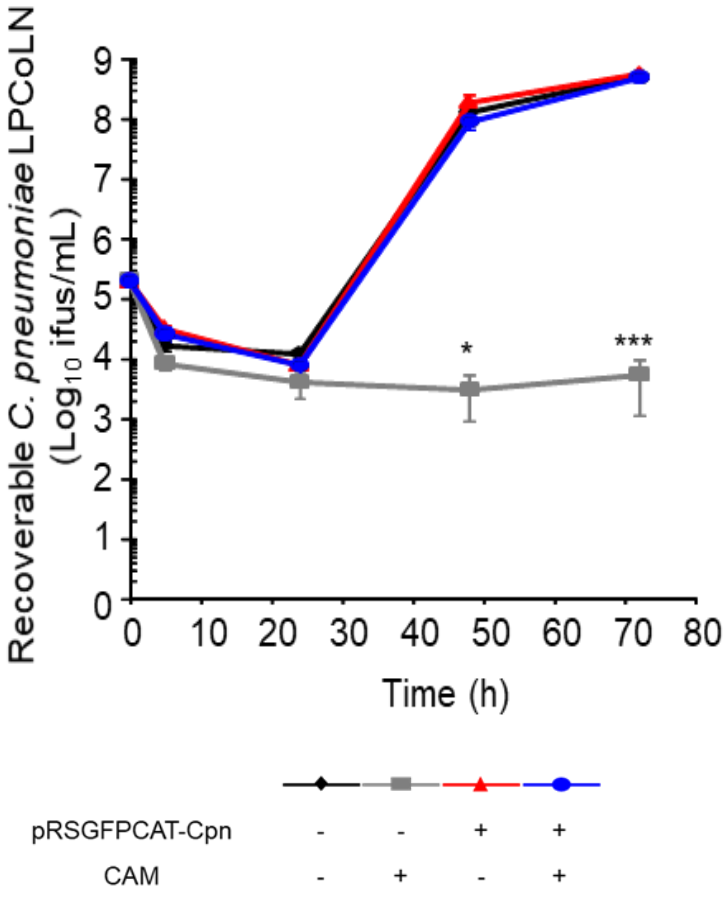

Figure 9: One-step growth curve of pRSGFPCAT-Cpn-transformed and untransformed *C. pneumoniae* LPCoLN.
Transformed and non-transformed *C. pneumoniae* LPCoLN were cultivated in HEp-2 cells with and without CAM. At 5, 24, 48 and 72 h.p.i. recoverable IFUs were determined. Growth characteristics under different conditions (gray, red, and blue graph) were compared to non-transformed and non-CAM treated *C. pneumoniae* LPCoLN (black graph) (n = 3, mean ± SEM; Sidak's multiple comparison; *: $p \leq 0.05$; ***: $p \leq 0.001$).

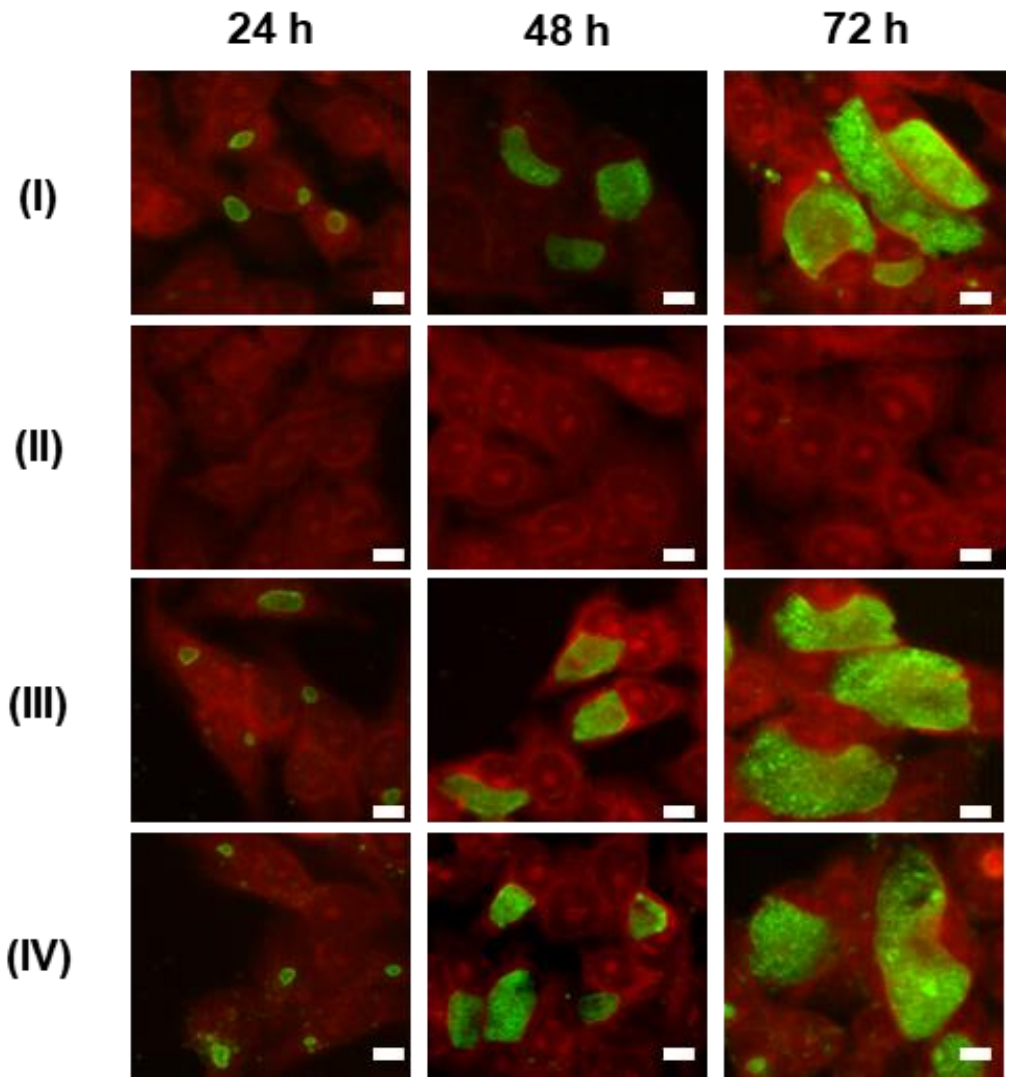

Figure 10: Immunofluorescence images of *C. pneumoniae* LPCoLN.
Transformed and non-transformed *C. pneumoniae* LPCoLN were cultivated in HEp-2 cells with and without CAM. At 24, 48 and 72 h.p.i. infected cells were fixed with methanol and stained. Afterwards, fluorescence images were taken with a fluorescence microscope. Chlamydial inclusions are shown in green and host cells (HEp-2) are shown in red. Images are representative of three independent experiments. White bars represent 10 µm.

(I) No transformation with pRSGFPCAT-Cpn and no CAM treatment
(II) No transformation with pRSGFPCAT-Cpn, but CAM treatment
(III) Transformation with pRSGFPCAT-Cpn, but no CAM treatment
(IV) Transformation with pRSGFPCAT-Cpn and CAM treatment

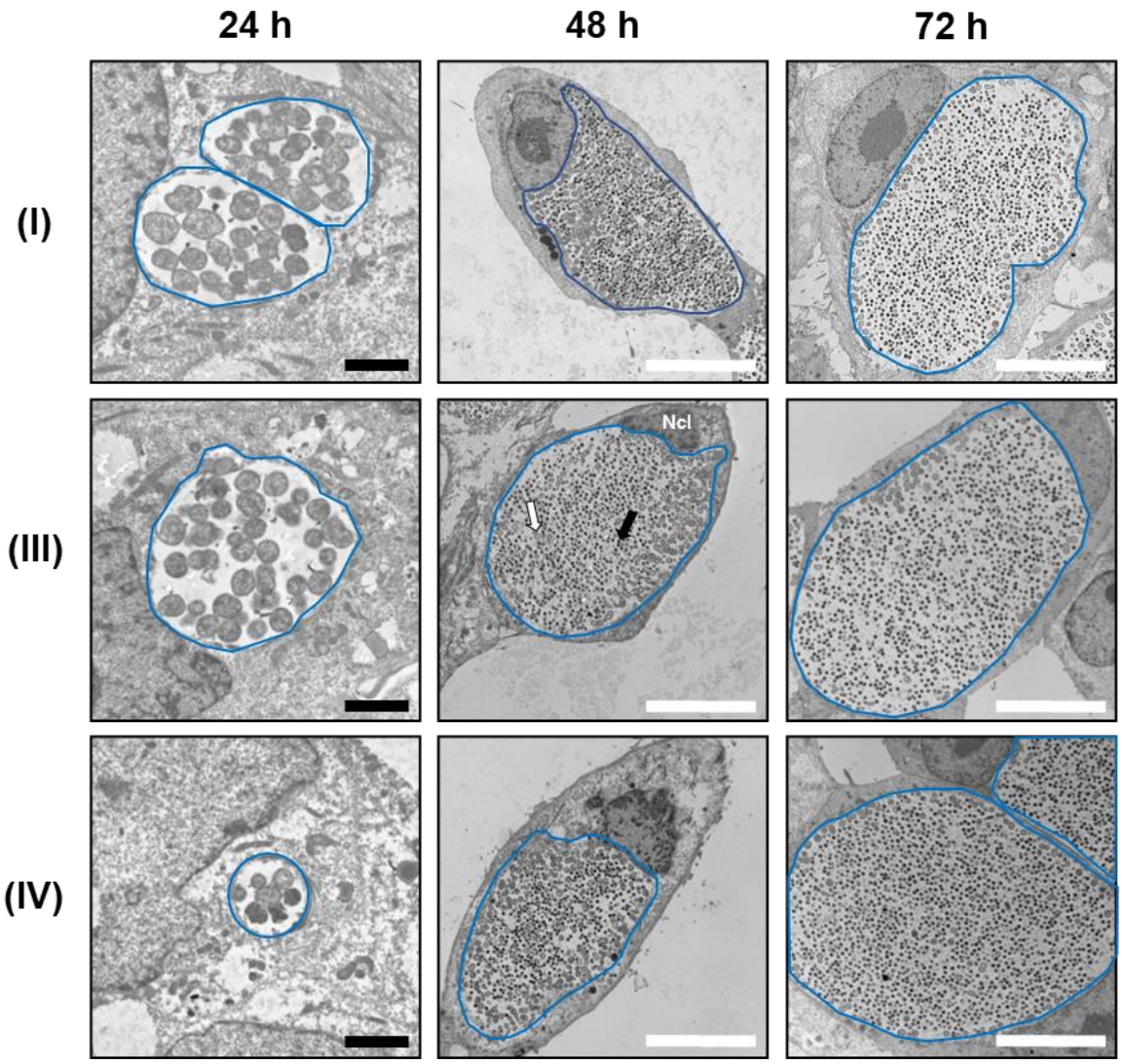

Figure 11: TEM images of *C. pneumoniae* LPCoLN.
Transformed and non-transformed *C. pneumoniae* LPCoLN were cultivated in HEp-2 cells with and without CAM. After 24, 48 and 72 h.p.i. TEM images were taken. Chlamydial inclusions are framed in blue. A black arrow shows an electron dense EB, and a white arrow shows a RB. Ncl abbreviation for nucleolus (host cell). Black bars represent 2 µm and white bars represent 10 µm.
(I) No transformation with pRSGFPCAT-Cpn and no CAM treatment
(III) Transformation with pRSGFPCAT-Cpn, but no CAM treatment
(IV) Transformation with pRSGFPCAT-Cpn and CAM treatment

It is well known that plasmids can be easily lost without antimicrobial selection pressure. Therefore, we next investigated the plasmid shuttle vector stability in transformed *C. pneumoniae* LPCoLN.

Transformed *C. pneumoniae* LPCoLN were cultivated in presence or absence of CAM for five passages (cf. figure 12). In this assay, the fluorescent RSGFP signal can be detected only in transformed *C. pneumoniae* LPCoLN. Whereas total number of transformed and untransformed *C. pneumoniae* LPCoLN were detected by immunofluorescence staining (IF). The ratio of RSGFP signal to IF signal was calculated. Our data shows that pRSGFPCAT-Cpn is stable after at least five passages even without CAM treatment. There are no statistically significant differences between both experimental conditions (n = 3, mean ± SEM, Sidak's multiple comparison) (cf. figure 12A).

In addition, representative images of *C. pneumoniae* LPCoLN infected HEp-2 cells from subculture 5 were taken (cf. figure 12B). These data indicates that pRSGFP-CAT-Cpn is stably maintained in transformed *C. pneumoniae* LPCoLN without the usage of CAM.

(A)

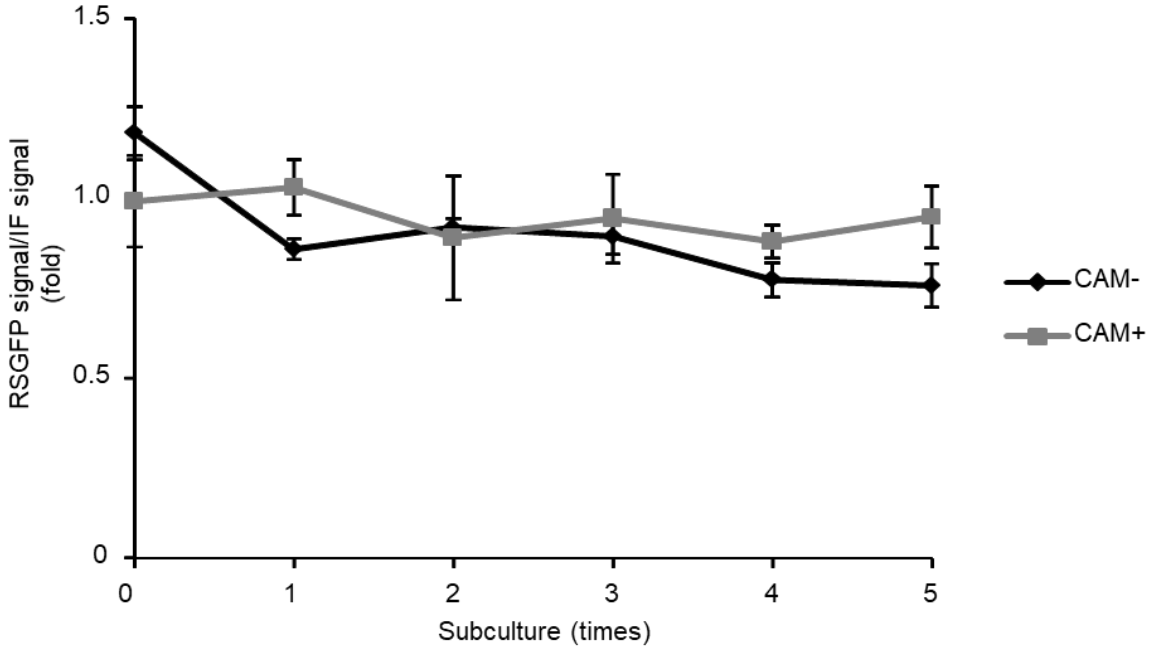

(B)

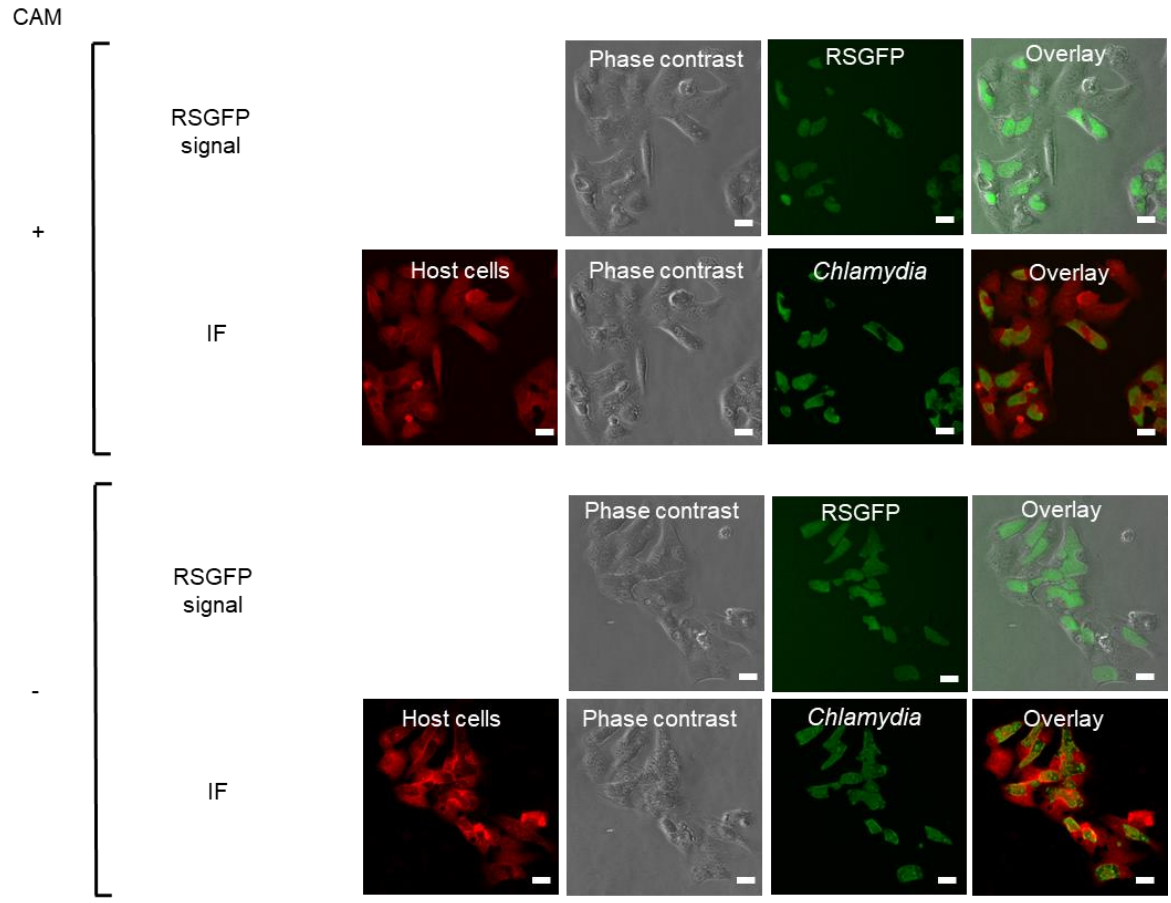

Figure 12: Plasmid stability of pRSGFPCAT-Cpn in *C. pneumoniae* LPCoLN. **(A)** After transformation with pRSGFPCAT-Cpn, *C. pneumoniae* LPCoLN was cultured in the presence (gray curve) or absence (black curve) of CAM for five passages. Using fluorescence microscopy, the ratio of RSGFP signal compared to the immunofluorescence (IF) signal was calculated. IF signal was generated using indirect immunofluorescence staining (Chlamydial-LPS antibodies (mouse) and anti-mouse antibodies (FITC-labeled)). (n = 3, mean ± SEM, Sidak's multiple comparison, no statistically significant difference).
(B) Representative fluorescence images of transformed *C. pneumoniae* LPCoLN either in presence (+) or absence (-) of CAM. The images were taken after 48 h.p.i. at passage 5. RSGFP signal was detected without previous staining. Stained IF images showing chlamydial inclusions (green) and host cells (red). White bars represent 20 µm.

6.3 pRSGFPCAT-Cpn allows genetic transformation of human isolates of C. pneumoniae

Human isolates of *C. pneumoniae* do not harbor an endogenous plasmid. Although the development of a successful transformation tool might be even more challenging, we next investigated transformation ability of clinically relevant human isolate *C. pneumoniae* CV-6. When pRSGFPCAT-Cpn was used, we observed a strong RSGFP signal within chlamydial inclusions in transformed *C. pneumoniae* CV-6 infected cells at 48 h.p.i. (cf. figure 13).

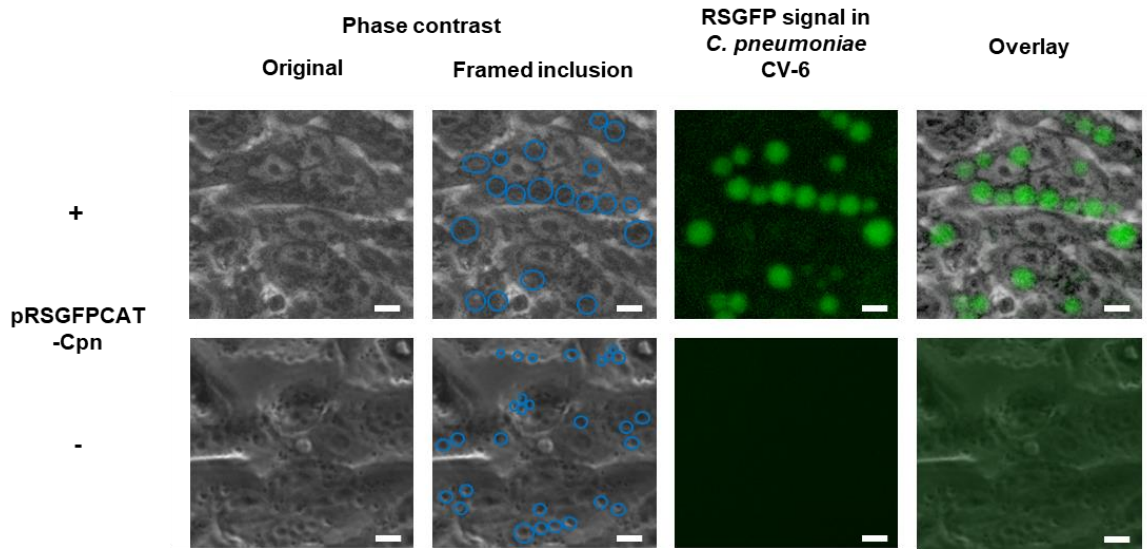

Figure 13: Representative images of successful transformed human isolate plasmid-free *C. pneumoniae* CV-6.
Successful transformation of human isolate *C. pneumoniae* CV-6 with pRSGFP-CAT-Cpn (+) compared to non-transformed *C. pneumoniae* CV-6 (-). The RSGFP signal (green) in chlamydial inclusions was detected after 48 h.p.i. using a fluorescence microscope. The images were taken in living host cells (HEp-2) without staining or fixing. Chlamydial inclusions were framed in blue. The scale bar represents 10 µm.

To exclude cross-contamination with other *Chlamydia* spp. whole genome sequencing of transformed *C. pneumoniae* CV-6 was performed. As the result, sequence homology between wild type *C. pneumoniae* CV-6 and transformed *C. pneumoniae* CV-6 was >99.99902%, indicating no accidentally cross-contamination with other *Chlamydia* spp. (cf. table 19). Performed DNA sequence analysis reveals that cardiovascular isolate *C. pneumoniae* CV-6 is 99.99829007% identical to *C. pneumoniae* CV-14 (cf. table 20).

Table 19: Whole genome sequence analysis between wild type *C. pneumoniae* CV-6 and transformed and RSGFP expressing *C. pneumoniae* CV-6 (transformation with pRSGFPCAT-Cpn).

***C. pneumoniae* CV-6 (transformed)**	
% Mapped reads	99.89
% Unmapped reads	0.11
% Reference bases covered	99.9998
Single nucleotide polymorphisms (SNPs)	9
Multi nucleotide polymorphisms (MNPs)	0
Indels < 5 bp	0
Inversions	0
% identity	99.99902058

Reads of transformed *C. pneumoniae* CV-6 was compared to wild type *C. pneumoniae* CV-6.

Table 20: **Whole genome sequence analysis between *C. pneumoniae* CV-6 and *C. pneumoniae* CV-14.**

***C. pneumoniae* CV-6**	
% Mapped reads	99.92
% Unmapped reads	0.08
% Reference bases covered	99.9993
Single nucleotide polymorphisms (SNPs)	8
Multi nucleotide polymorphisms (MNPs)	0
Indels < 5 bp	2
Inversions	0
% identity	99.99829007

Reads of *C. pneumoniae* CV-6 was compared to *C. pneumoniae* CV-14.

Plasmid DNA sequencing was also performed to ensure that the correct plasmid shuttle vector was used for transformation and that no genetic recombination took place. This assay showed 100% identity between the original pRSGFPCAT-Cpn and the plasmids isolated from transformed *C. pneumoniae* CV-6 (pRSGFPCAT-Cpn). This indicates that human isolate plasmid-free *C. pneumoniae* CV-6 was successfully transformed using the novel pRSGFPCAT-Cpn (derived from *C. pneumoniae* N16) without recombination.

Next, we performed recovery assays to investigate whether pRSGFPCAT-Cpn has an impact on chlamydial growth or bacterial morphology (cf. figure 14,15 and 16).

The recovery assay showed similar growth characteristics between transformed and wild type *C. pneumoniae* CV-6 without CAM treatment. There is also no significant

difference in growth characteristics of transformed *C. pneumoniae* CV-6 in the presence or absence of CAM (cf. figure 14).

Additional immunofluorescence and TEM analysis show that the transformation with pRSGFPCAT-Cpn has no effect on chlamydial morphology (cf. figure 15 and 16).

No additional TEM images were taken from CAM treated wild type *C. pneumoniae* CV-6. In further experiments, RSGFP espression in *C. pneumoniae* CV-6 was dedected at least for 5 passages, indicating that pRSGFPCAT-Cpn was stably maintained (cf. figure 17).

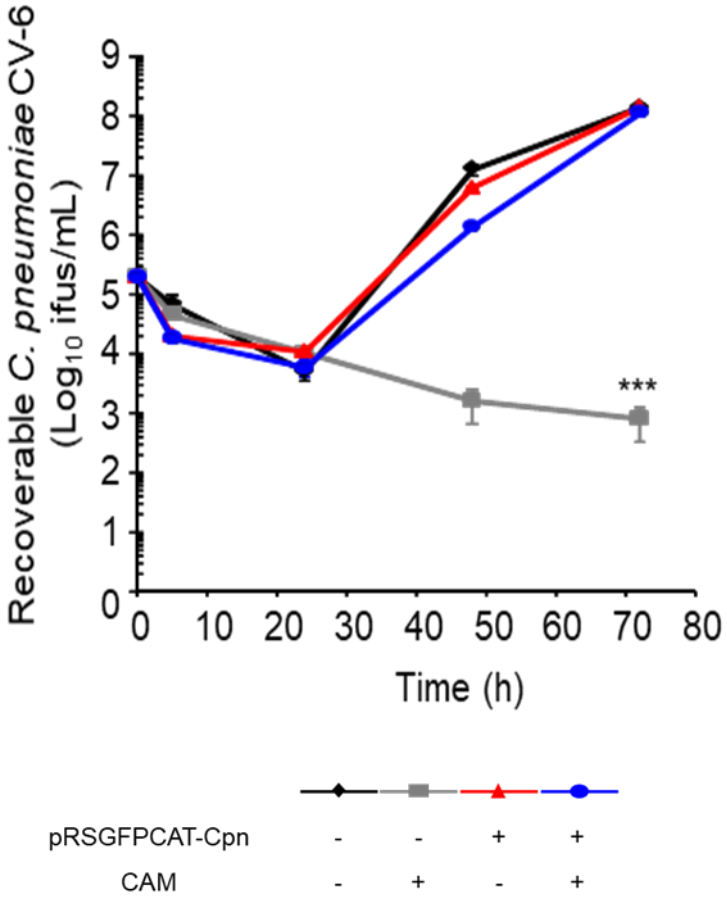

Figure 14: One-step growth curve of pRSGFPCAT-Cpn-transformed and untransformed *C. pneumoniae* CV-6.
Transformed and non-transformed *C. pneumoniae* CV-6 were cultivated in HEp-2 cells with and without CAM. After 5, 24, 48 and 72 h.p.i. recoverable IFUs were determined and illustrated in growth curves. Growth characteristics under different conditions (gray, red, and blue graph) were compared to non-transformed and non-CAM treated *C. pneumonaie* CV-6 (black graph) (n = 4, mean ± SEM; Sidak's multiple comparison; ***: $p \leq 0.001$).

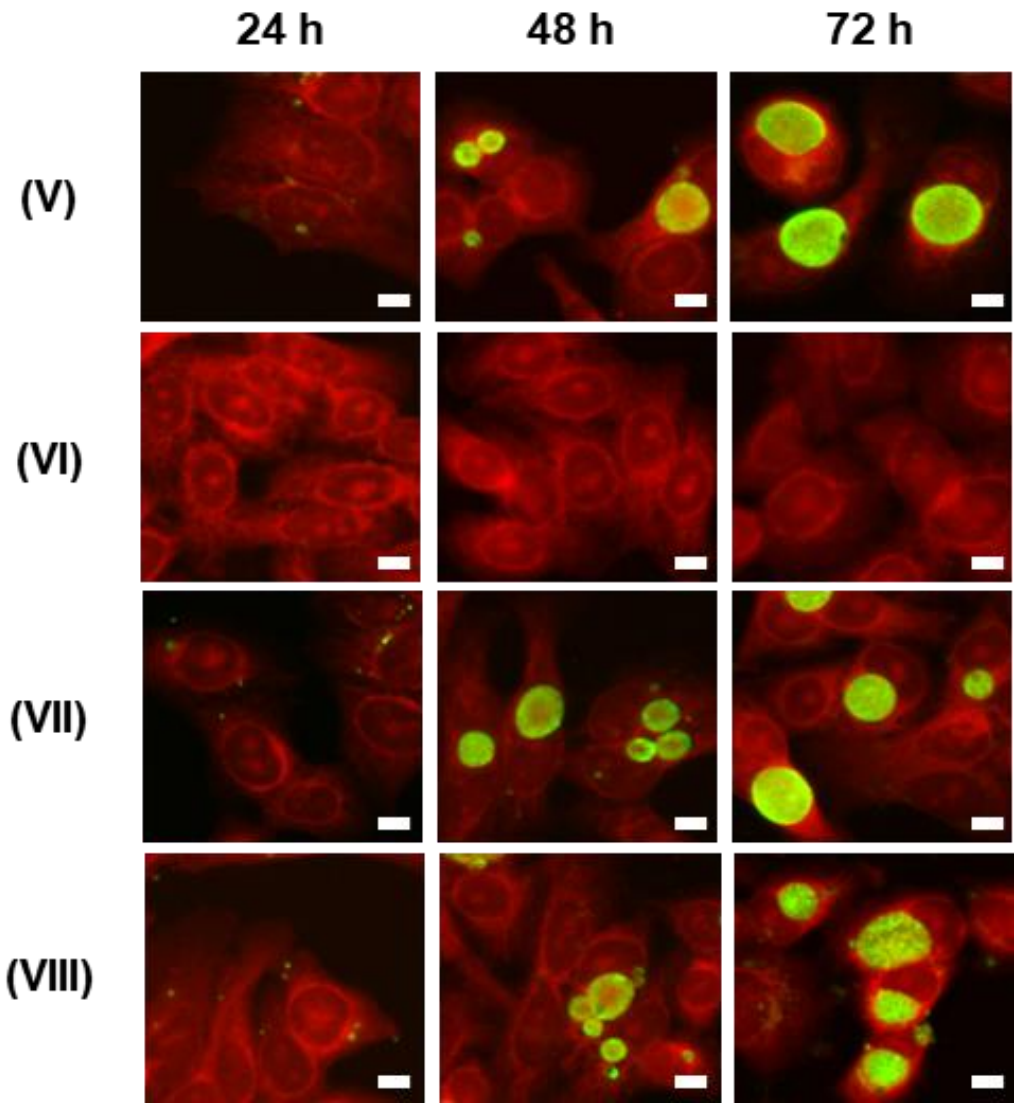

Figure 15: Immunofluorescence images of *C. pneumoniae* CV-6.
Transformed and non-transformed *C. pneumoniae* CV-6 were cultivated in HEp-2 cells with and without CAM. After 24, 48 and 72 h.p.i. infected cells were fixed with methanol and stained. Afterwards fluorescence images were taken with a fluorescence microscope. Chlamydial inclusions are shown in green and host cells (HEp-2) are shown in red. Images are representative of three independent experiments. White bars represent 10 µm.

(V) No transformation with pRSGFPCAT-Cpn and no CAM treatment
(VI) No transformation with pRSGFPCAT-Cpn, but CAM treatment
(VII) Transformation with pRSGFPCAT-Cpn, but no CAM treatment
(VIII) Transformation with pRSGFPCAT-Cpn and CAM treatment

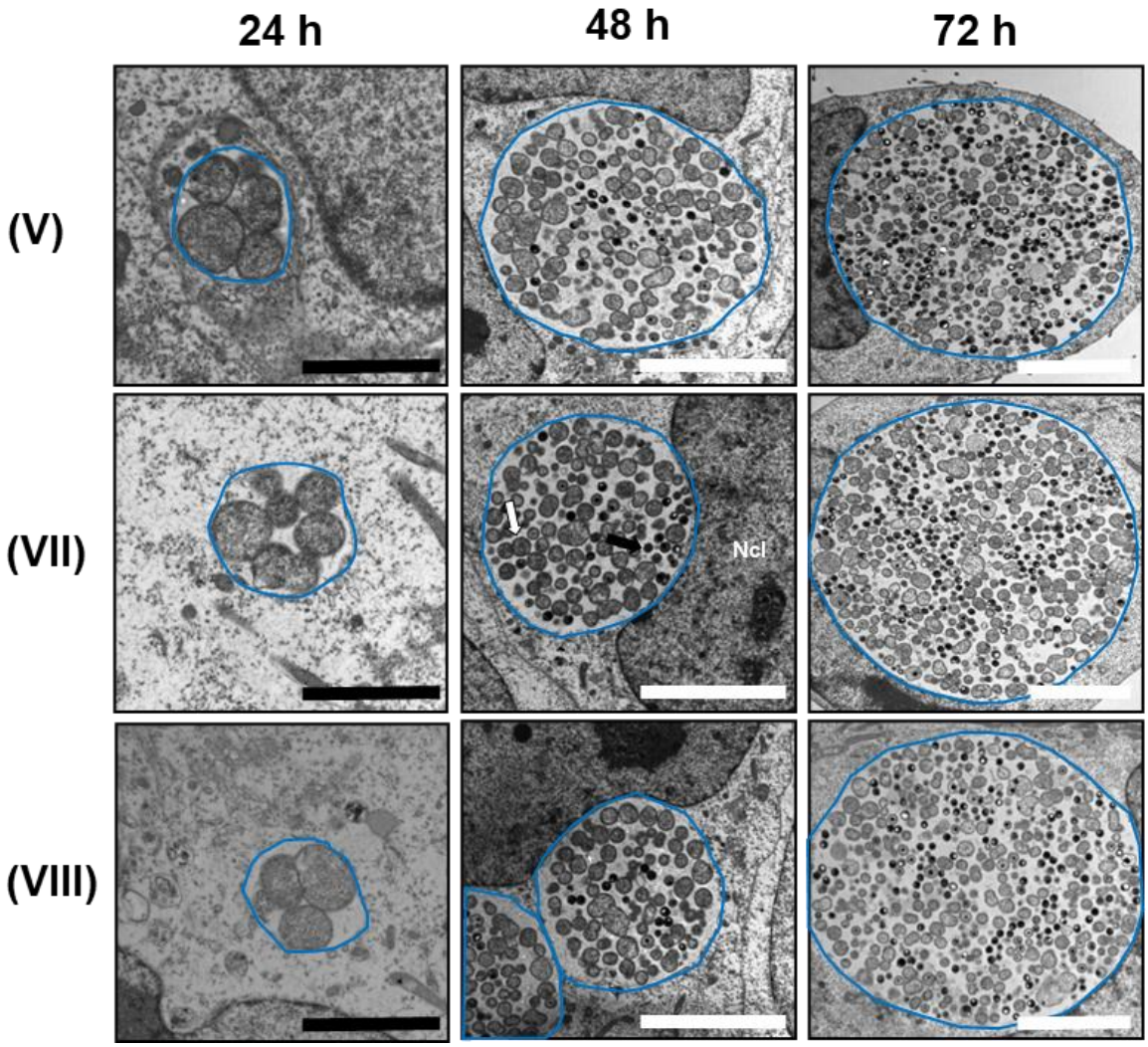

Figure 16: TEM images of *C. pneumoniae* CV-6.
Transformed and non-transformed *C. pneumoniae* CV-6 were cultivated in HEp-2 cells with and without CAM. After 24, 48 and 72 h.p.i. TEM images were taken. Chlamydial inclusions are framed in blue. A black arrow shows an electron dense EB and a white arrow shows a RB. Ncl abbreviation for nucleolus (host cell). Black bars represent 2 µm and white bars represent 5 µm.
(V) No transformation with pRSGFPCAT-Cpn and no CAM treatment
(VII) Transformation with pRSGFPCAT-Cpn, but no CAM treatment
(VIII) Transformation with pRSGFPCAT-Cpn and CAM treatment

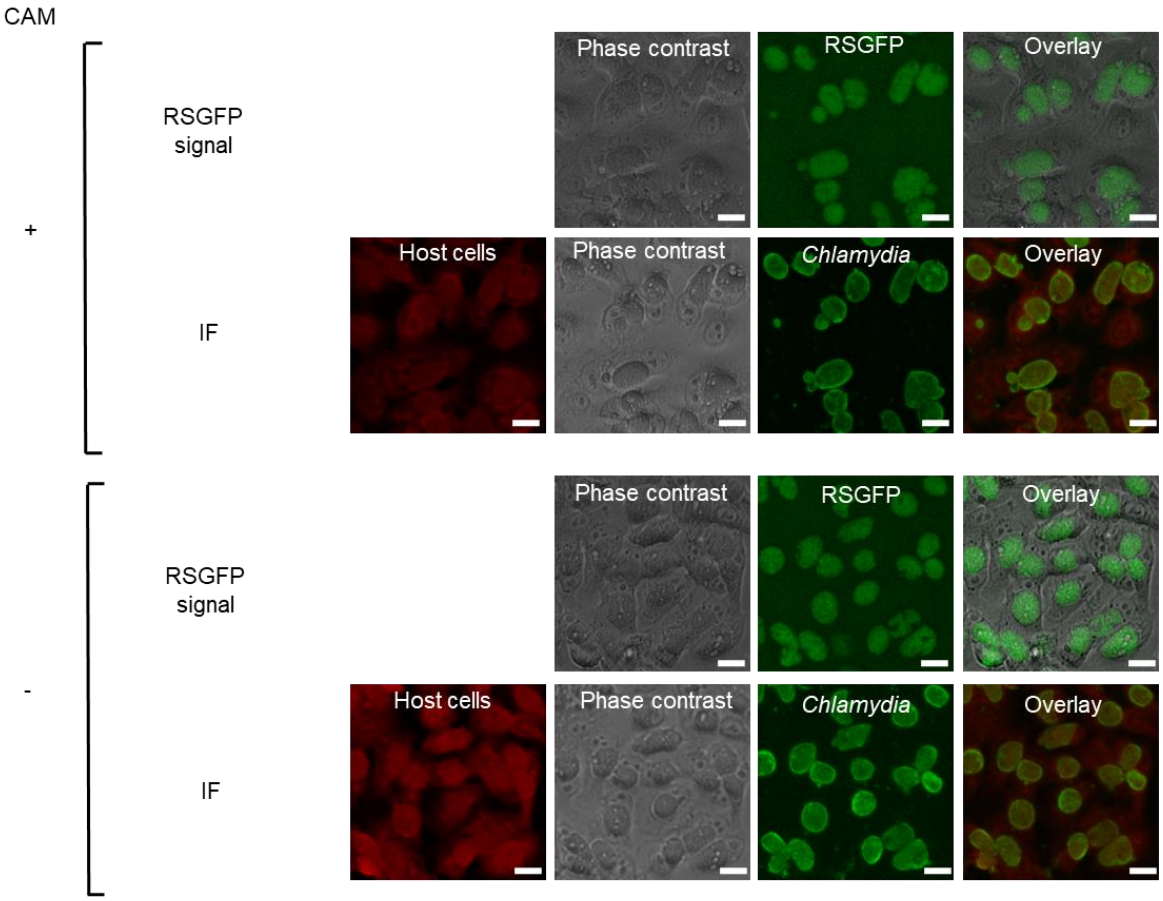

Figure 17: Representative fluorescence images of transformed *C. pneumoniae* CV-6 either in presence (+) or absence (-) of CAM.
The images were taken after 72 h.p.i. at passage 5. RSGFP signal was detected without previous staining. Stained immunofluorescence (IF) images showing chlamydial inclusions (green) and host cells (red). White bars represent 20 µm.

6.4 pRSGFPCAT-Cpn overcomes plasmid tropism

In our experiments we demonstrated that pRSGFPCAT-Cpn can be used for transformation of *C. pneumoniae*. Due to plasmid tropism in chlamydiae, it has been demonstrated that *Chlamydia* spp. could be transformed only if the plasmid shuttle vector is constructed with the same backbone as the plasmid harbored in the identical species. To understand availability and limitation of our shuttle vector, we next investigated the plasmid tropism in chlaymdiae.

When other *Chlamydia* spp. such as *C. felis*, *C. muridarum*, *C. caviae*, *C. abortus* C18/98, *C. pecorum* 14DC102 and *C. trachomatis* L2 were transformed with pRSGFPCAT-Cpn, a strong RSGFP signal was detected in *C. felis* N.I. ("not identified") (cf. figure 18A) but not in other tested chlamydiae (cf. table 21). Whole genome analysis of *C. felis* N.I. showing a high similarity of 99.99% between *C. felis* N.I. and *C. felis* Fe/C-56 (cf. table 22). Successful transformation was also observed in plasmid-barring *C. felis* Cello (cf. figure 18B) and the plasmid-free *C. felis* 02DC26 (cf. figure 18C).

Table 21: Transformation results of various *Chlamydia* spp.

Species	Strain	Host	Wild type plasmid	Expression of RSGFP
Chlamydia abortus	C18/98 (B577)	Sheep	-	-
Chlamydia caviae	03DC25 (GPIC)	Guinea pig	+	-
Chlamydia felis	Not identified (N.I)	N.I.	+	+
Chlamydia felis	02DC26 (Cf02-23)	Cat	-	+
Chlamydia felis	Cello	Cat	+	+
Chlamydia muridarum	MoPn/Nigg	Mouse	+	-
Chlamydia pecorum	14DC102 (E58)	Cattle	-	-
Chlamydia pneumoniae	LPCoLN	Koala	+	+
Chlamydia pneumoniae	CV-6	Human	-	+
Chlamydia trachomatis	L2 (25667R)	Human	-	-

Listed *Chlamydia* spp. were transformed with the pRSGFPCAT-Cpn plasmid shuttle vector. Afterwards the RSGFP fluorescence signal could be detected (+) or not (-). Some *Chlamydia* spp. contain an extrachromosomal wild type plasmid. The plasmid presence is illustrated in this table with (+) for containing and (-) for non-containing wild type plasmid.

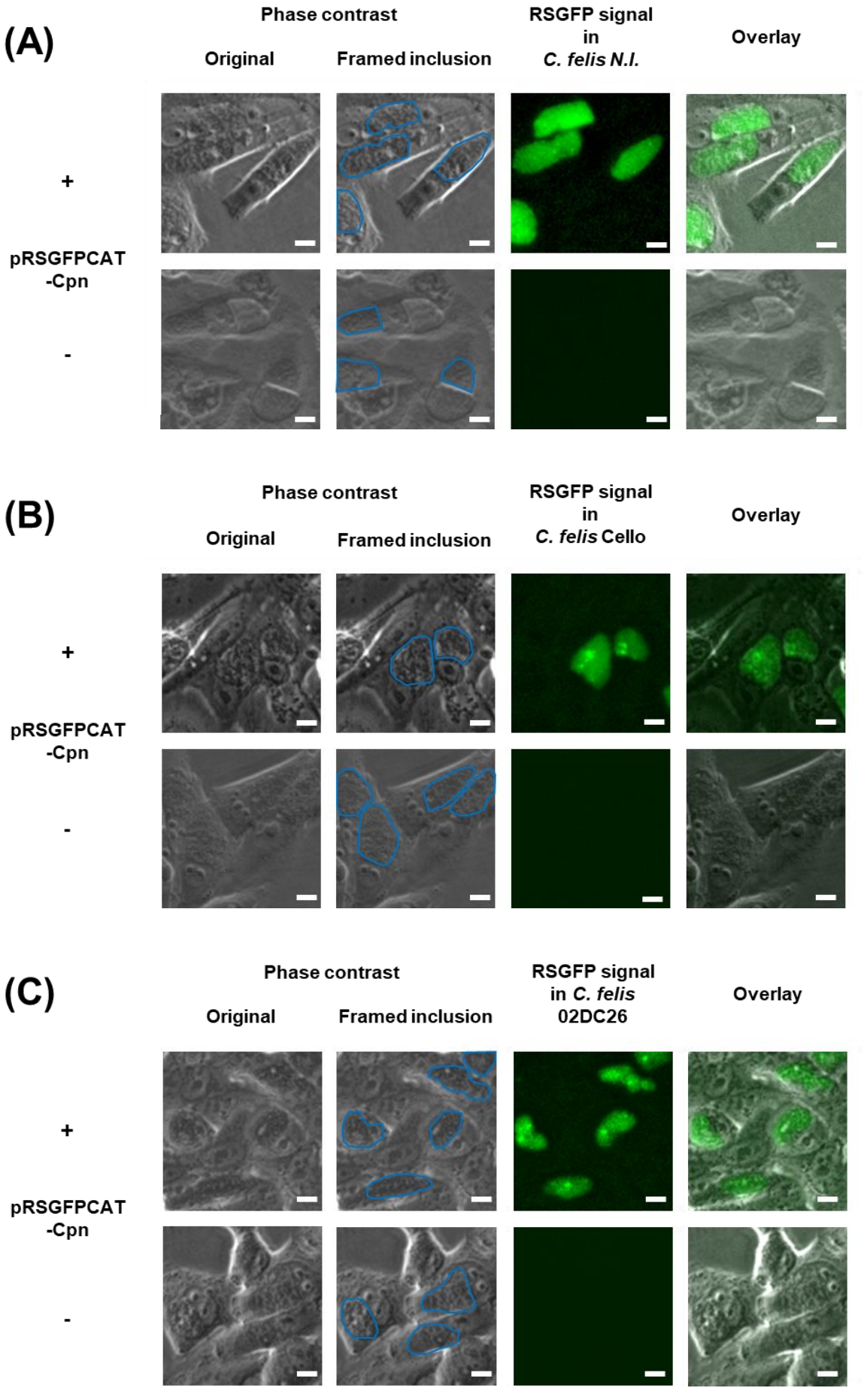
(A)
Phase contrast
Original
Framed inclusion
RSGFP signal in C. felis N.I.
Overlay
+
pRSGFPCAT -Cpn
-
(B)
Phase contrast
Original
Framed inclusion
RSGFP signal in C. felis Cello
Overlay
+
pRSGFPCAT -Cpn
-
(C)
Phase contrast
Original
Framed inclusion
RSGFP signal in C. felis 02DC26
Overlay
+
pRSGFPCAT -Cpn
-

Figure 18: Representative images of transformed *C. felis*
(A) Transformation of *C. felis* N.I. with pRSGFPCAT-Cpn (+) compared to non-transformed *C. felis* N.I. (-).
(B) Transformation of *C. felis* Cello with pRSGFPCAT-Cpn (+) compared to non-transformed *C. felis* Cello (-).
(C) Transformation of animal isolate *C. felis* 02DC26 with pRSGFPCAT-Cpn (+) compared to non-transformed *C. felis* 02DC26 (-).
The RSGFP signal (green) in chlamydial inclusions was detected after 48 h.p.i. using a fluorescence microscope. The images were taken in living host cells (HEp-2) without staining or fixing. Chlamydial inclusions were framed in blue. The scale bar represents 10 µm.

Table 22: Whole genome sequence analysis between *C. felis* N.I. and *C. felis* Fe/C-56.

***C. felis* N.I.**	
% Mapped reads	99.97
% Unmapped reads	0.03
% Reference bases covered	99.9956
Single nucleotide polymorphisms (SNPs)	93
Multi nucleotide polymorphisms (MNPs)	0
Indels >= 5 bp	1
Indels <= 5 bp	10
Inversions	0
% identity	99.98533748

Reads of *C. felis* N.I. was compared to *C. felis* Fe/C-56.

Further plasmid sequence analyses show that pRSGFPCAT-Cpn isolated from transformed *C. felis* is 100% identical compared to the original pRSGFPCAT-Cpn. This result indicates that the correct plasmid shuttle vector was used for transformation and that no genetic recombination occurred to cross species barrier.

To investigate whether the plasmid species barrier is not valid in *C. felis*, transformation experiment was also performed using *C. trachomatis*-derived plasmid shuttle vector pGFP::SW2 (86). No RSGFP signal was detected when pGFP::SW2 was used for the transformation of *C. felis*. Due to these results further plasmid DNA sequence analyses were performed comparing the plasmid of *C. felis* N.I. (pCfelis) to the plasmids of *C. trachomatis* L2 (pL2), *C. pneumoniae* N16 (pCpnEI) and *C. pneumoniae* LPCoLN (pCpnKo). This analysis revealed that pL2, pCpnEI, and pCpnKo have a plasmid homology of approximately 60% compared with pCfelis (cf. table 23).

Table 23: **Plasmid DNA sequence homology of *C. felis* compared to *C. trachomatis* and *C. pneumoniae.***

Species	Strain	Plasmid	all CDS	CDS 1	CDS 2	CDS 3	CDS 4	CDS 5	CDS 6	CDS 7	CDS 8
C. felis	N.I.	pCfelis	100	100	100	100	100	100	100	100	100
C. trachomatis	L2	pL2	62	62	61	59	66	65	72	60	62
C. pneumoniae	LPCoLN	pCpnKo	68	71	64	67	77	64	77	71	62
C. pneumoniae	N16	pCpnEI	65	47	67	68	77	64	76	70	62

Homology is indicated in percent (%). Human isolate *C. pneumoniae* are not analyzed due to their lack of extrachromosomal plasmids.

7 Discussion

Infections with *Chlamydia* spp. are quite common worldwide and cause severe diseases in humans (3). To understand the complex molecular mechanism in chlamydial pathogenesis, various research groups have made attempts to develop new molecular tools for the genetic modification of chlamydiae. Since Wang *et al.* (86) established a suitable transformation protocol using plasmid shuttle vectors for *C. trachomatis* L2 in 2011, several modified methods were developed for *C. trachomatis*. This fundamental discovery opened a new era of chlamydial research (46). Recent studies demonstrate that the *C. trachomatis*-derived plasmid shuttle vector called pGFP::SW2 could be used not only for transformation of *C. trachomatis* L2 and the plasmid-free strain L2R but also for plasmid-free serovar D and F (86,103–106). Nevertheless, transformation of other *Chlamydia spp*. was still challenging and has not been succeeded using pGFP::SW2. Song *et al.* demonstrated that other *Chlamydia spp*. such as *C. muridarum* can be transformed when the backbone of the chlamydial plasmid shuttle vector is constructed from the same chlamydial species (95), indicating the presence of a chlamydial plasmid tropism. Due to this, universal transformation protocols are not applicable for all chlamydiae. Therefore, we focused on the development of a new transformation protocol for *C. pneumoniae.*

7.1 Genetic transformation of C. pneumoniae

To establish a transformation protocol for *C. pneumoniae*, we developed a new plasmid shuttle vector called pRSGFPCAT-Cpn. In our approach, we constructed pRSGFPCAT-Cpn using the plasmid of the equine *C. pneumoniae* N16 and the vector pRSGFPCAT (cf. figure 5). Because the guidelines of the World Health Organization (WHO) recommends β-lactam antibiotics, such as amoxicillin, as a treatment option for infections with *C. trachomatis* in pregnant women (107) we used CAM as a suitable selection marker. This precautionary measure was taken to avoid the emergence of β-lactam antibiotic resistant strains.

The plasmid isolated from *C. pneumoniae* N16 called pCpnEI has a similar size and arrangement of coding sequences (CDSs) compared to other *Chlamydia* spp. (52,91,108,109). Nevertheless, it is slightly different due to a deletion within the CDS1. The deletion on pCpnEI resulted in the formation of two smaller CDSs named

CDS1A and CDS1B (91). The changes at CDS1, however, do not appear to have a significant impact on *C. pneumoniae* N16 replication.

Using the new constructed pRSGFPCAT-Cpn, we demonstrated successful transformation and RSGFP expression in plasmid-bearing animal isolate *C. pneumoniae* LPCoLN (cf. figure 8). Since *C. pneumoniae* can express RSGFP using meningococcal class I protein promoter, we suggest that a promoter sequence is not selective for *C. pneumoniae*.

While zoonic *C. pneumoniae* harbors plasmids, all human isolates of *C. pneumoniae* do not possess an extrachromosomal plasmid. It has been hypothesized that human isolates of *C. pneumoniae* evolved from animal isolates, resulting in a reduced genome and the loss of plasmids (50,108). It is supposed that human isolate *C. pneumoniae* lost their plasmids during chlamydial evolution since they are not crucial for chlamydial survival or dissemination (108).

Although some differences between animal and human isolates of *C. pneumoniae* were found in the genome sequence, it has been demonstrated that they are evolutionary closely related (50,108). Therefore, we assumed that the *C. pneumoniae* N16-derived plasmid shuttle vector pRSGFPCAT-Cpn could also be used for the transformation of human isolates of *C. pneumoniae*.

In fact, we could demonstrate a successful transformation of human cardiovascular isolate *C. pneumoniae* CV-6 using pRSGFPCAT-Cpn (cf. fig. 13). Following whole genome sequence analyses between wild type *C. pneumoniae* CV-6 and transformed *C. pneumoniae* CV-6 showed that both samples are nearly identical (99.99%, cf. table 19). Hence, cross-contamination with other *Chlamydia* spp. could be excluded in our study. Furthermore, DNA sequence results of pRSGFPCAT-Cpn isolated from transformed *C. pneumoniae* CV-6 revealed no insertions and deletions compared to the original DNA sequence of pRSGFPCAT-Cpn. This result indicates that genetic recombination of the plasmid is not required for successful transformation of human isolate *C. pneumoniae* using animal isolate derived plasmid shuttle vector. Performed whole genome sequence analyses revealed high sequence homology between CV-6 and other cardiovascular *C. pneumoniae* strain named CV-14 (cf. table 20). Therefore, we assume that our shuttle vector could also be utilized for other cardiovascular isolates of *C. pneumoniae*.

After successful transformation, we showed in additional experiments that pRSGFPCAT-Cpn has no impact on chlamydial growth (cf. figure 9 and 14) or morphology

(cf. figure 10, 11, 14 and 15). Furthermore, we even observed a strong RSGFP signal without antibiotic selective pressure at least for five passages in the plasmid stability test (cf. figure 12). This indicates that antibiotic selection is not mandatory and further functional analyses using pRSGFPCAT-Cpn can be performed without CAM treatment.

Summing up, our results show that the novel plasmid shuttle vector system using *C. pneumoniae-derived* pRSGFPCAT-Cpn can transform plasmid harboring animal isolate *C. pneumoniae* LPCoLN as well as plasmid-free human isolate *C. pneumoniae* CV-6. Furthermore, our plasmid shuttle vector is stable even in the absence of antibiotics (CAM) and have no impact on chlamydial growth and morphological characteristics. Next, we were interested if pRSGFPCAT-Cpn can deal with plasmid tropism and is able to transform other *Chlamydia* spp. besides *C. pneumoniae*.

7.2 Overcoming chlamydial plasmid tropism

Recent studies showed that chlamydial plasmid shuttle vectors must contain the chlamydial backbone of the endogenous plasmid to overcome plasmid species barrier (95). Wang *et al.* demonstrated that the CDS2 region located on chlamydial plasmid is essential for plasmid maintenance and is linked to plasmid tropism (97). To deepen our knowledge of chlamydial plasmid tropism, we next investigated the transformation capability of eight other *Chlamydia* spp. using pRSGFPCAT-Cpn. In this study, we could not observe RSGFP expression in *C. abortus, C. caviae, C. muridarum, C. pecorum* or *C. trachomatis.* Astonishingly pRSGFPCAT-Cpn transformation was successful in three different strains of *C. felis* including *C. felis* N.I., *C. felis* Cello and *C. felis* 02DC26 (cf. table 21 and figure 18). All transformants showed strong RSGFP signals without previous staining (cf. figure 18).

C. felis is taxonomically close related to *C. pneumoniae* (110). It is an intracellular Gram-negative bacterium that infects cats and causes conjunctivitis, rhinitis and pneumonia (34,98,110,111). There are also several case reports describing conjunctivitis in human caused by *C. felis.* These reports indicate that the pathogen might be transmitted from patient's pet infected with *C. felis* (112).

First genetic analyzes showed that *C. felis* Fe/C-56 has a 1,166,239-bp large genome containing 1005 protein-coding genes and harbors an extrachromosomal 7,552-bp plasmid called pCfe1 (110). Whole genome sequence analysis of *C. felis*

N.I. which were used in our experiments revealed 99.99% similarity compared to *C. felis* Fe/C-56 (cf. table 22).

While *C. felis* Fe/C-56 as well as Pring and Cello harbor plasmids (34,98), some other *C. felis* strains such as 02DC26 (Cf02-23) or Backer do not carry such extrachromosomal plasmids (34,98). Since we could detect a strong RSGFP signal after transformation in both, *C. felis* Cello (plasmid carrying) and *C. felis* 02DC26 (non-plasmid-carrying) we suggest that the endogenous plasmid does not influence the transformation of *C. felis*.

The sequence analysis of transformed *C. felis* derived pRSGFPCAT-Cpn revealed no genetic recombination between pRSGFPCAT-Cpn and wild type *C. felis* plasmids. While a plasmid backbone of the same chlamydial species or recombination of CDS2 regions were required for successful transformation (97), these factors were not needed for the transformation of *C. felis* when pRSGFPCAT-Cpn was used. This indicates that pRSGFPCAT-Cpn exceptionally overcame the plasmid species barrier in *C. felis*.

To exclude the possibility of an unknown transformation ability of *C. felis* strains we also performed transformation experiments using *C. felis* and the *C. trachomatis*-derived plasmid shuttle vector pGFP::SW2 (104). However, our experiments showed that *C. felis* do not express RSGFP when pGFP::SW2 is used for transformation. Further plasmid analyses showed that the endogenous plasmids of *C. trachomatis* and *C. pneumoniae* reveal respectively a homology around 60% compared to the endogenous plasmid of *C. felis* (cf. table 23). Nevertheless, only the *C. pneumoniae*-derived plasmid shuttle vector resulted in the expression of RSGFP in *C. felis*. Taking together those results show that an unidentified biological mechanism promotes the transformation ability of *C. felis* and further investigations are needed. However, our results showed that pRSGFPCAT-Cpn can be transformed in two different *Chlamydia* spp. which imply that horizontal gene transfer among chlamydiae via plasmids might be possible.

7.3 Horizontal gene transfer among chlamydiae

Genes can be transferred between prokaryotes facilitated by plasmids, bacteriophages, or viruses. This phenomenon is called horizontal gene transfer and plays an important role in bacterial evolution. Horizontal gene transfer is a quite common ability of prokaryotic organism and allows the exchange of various genes including

antibiotic resistance genes. Moreover, it plays a key role in bacterial genome evolution and development of survival mechanisms due to environmental challenges (113,114).

Previous studies suggest that horizontal gene transfer among chlamydiae is possible *in vitro*. For instance, it has been shown that chlamydial inclusion can fuse during coinfection demonstrating that two *Chlamydia* spp. can have direct contact during infection (115). In addition, it has been demonstrated that chlamydiae can insert antibiotic resistance genes into the chlamydial genome by genetic recombination (115,116). Since our *C. pneumoniae*-derived plasmid shuttle vector pRSGFPCAT-Cpn can transform different *Chlamydia* spp. (*C. pneumoniae* and *C. felis*), we suggest that horizontal gene transfer via plasmids among different *Chlamydia* spp. can also potentially occur in nature.

Our results as well as the findings of previous studies show that horizontal gene transfer among *C. felis* and *C. pneumoniae* might be possible and even relevant for public health. Considering the high percentage (around 33%) of domestic cat population worldwide (117,118), the case reports about human isolate *C. felis* (112), and the usage of antibiotics in veterinary medicine (119), it can be hypothesized that antibiotic resistance genes located on plasmids might also be exchanged among chlamydiae. In the end, those gene exchanges could complicate the treatment of chlamydial infections in clinical daily routine.

In summary, the novel pRSGFPCAT-Cpn plasmid shuttle vector can be used to overcome chlamydial plasmid tropism and can be expressed in *C. felis*. Hence, it can be speculated that horizontal gene transfer via plasmids between *C. felis* and *C. pneumoniae* might occur in nature. Since this event would have drastic effects on public health, further studies are needed to verify this assumption.

7.4 Outlook

Novel plasmid shuttle vectors for chlamydiae can be used for various purposes (46). Recent studies have shown, for example, that GFP expressing *C. trachomatis* can be quantitatively monitored using fluorescence microscopy and flow cytometry to investigate the developmental life cycle of chlamydiae (120). Furthermore, another study showed that luciferase-expressing *C. muridarum* can be monitored in infected mice using a whole body bioluminescence imaging approach (121). These examples demonstrate impressively how plasmid shuttle vectors can be used to monitor

chlamydial infections *in vitro* as well as *in vivo*. Our novel plasmid shuttle vector pRSGFPCAT-Cpn can also be used for similar observation experiments in *C. pneumoniae* and even in *C. felis*.

Since chlamydial genome and endogenous plasmids have a major impact on their infection behavior, metabolism, and pathogenesis, substantiated knowledge about chlamydial plasmids and genome is essential. Song *et al.* (94) and Gong *et al.* (103) uncovered unknown functions of chlamydial plasmid encoded genes using *C. trachomatis*-derived shuttle plasmid vectors such as pGFP::SW2 (86) or pBRCT (94). They showed that plasmid encoded genes are associated with various functions such as chlamydial metabolism, virulence or plasmid maintenance and replication (90–92,94,95,103) (cf. table. 2). Due to the lack of genetic tools for *C. pneumoniae* it has not been elucidated whether these plasmids encoded genes have similar functions in *C. pneumoniae*. Since our DNA sequence analyses of chlamydial plasmids revealed disparities among various *Chlamydia* spp. (cf. table 18), we assume that these differences might affect CDS functions in *C. pneumoniae*. To elucidate CDS functions in *C. pneumoniae*, individual CDS deletion vectors can be constructed, as shown in a previous study (94), and effects of deleted CDS can be assessed after transformation. To conduct this assay, overlapping extension PCR cloning can be used to generate deletion vectors of pRSGFPCAT-Cpn without the need of restriction enzymes and ligases (122,123).

In the last years, the modification of the chlamydial genome has also been focused in different studies (46). Chemical random mutagenesis in chlamydial genome was performed using ethyl methanesulfonate (EMS) to investigate the effect of specific genes on chlamydial phenotype (124). Furthermore, targeted mutagenesis was also established in *C. trachomatis* using plasmid shuttle vectors. Johnson and Fisher used a modified TargeTron™ system for *C. trachomatis* to deactivate the *incA* gene located on chlamydial genome (125). Mueller *et al.* developed a *C. trachomatis*-derived plasmid shuttle vector that can be used for targeted fluorescence-reported allelic exchange mutagenesis (FRAEM) in chlamydiae (126). Both approaches would be barely conceivable without the use of chlamydial plasmid shuttle vectors. While various novel approaches of genetic modification were established for *C. trachomatis*, progress of such a technique is far behind in *C. pneumoniae*. By establishing a well-working transformation protocol for *C. pneumoniae,* first steps have

been conducted and our novel plasmid shuttle vector pRSGFPCAT-Cpn can serve as the basis for the development of new molecular tools for *C. pneumoniae*.

These new molecular tools can also be used for investigating tissue tropism in *C. pneumoniae*. Recent studies demonstrated that genes of the *omp* (outer-membrane proteins) family, *pmp* (polymorphic membrane proteins) family or *Inc* (inclusion membrane proteins) family are linked to chlamydial tissue tropism in *C. trachomatis* (127). Genetic factors linked to tissue tropism such as *ompA, pmp20* or *ygeD-urk* are also identified in *C. pneumoniae* (49,128). In addition, nsSNPs were found to be also associated with tissue tropism of *C. pneumoniae* (49). Interestingly, nsSNPs were found in nine genes related to chlamydial RB-to-EB differentiation, inclusion membrane development, chlamydial stress response, or metabolism. Applying gain and loss function that can be manipulated by the plasmid shuttle vector system and mutagenized *C. pneumoniae,* it is possible to explore *C. pneumoniae* tissue tropism and gain new insights.

Many new genetic tools for *C. trachomatis* are available since first transformation attempts were published. These approaches can now be adapted to *C. pneumoniae* using pRSGFPCAT-Cpn, launching a new era of chlamydial research.

7.5 Conclusion

For the genetic modification of the obligate intracellular *C. pneumoniae* we successfully constructed a *C. pneumoniae*-derived shuttle plasmid vector we called pRSGFCAT-Cpn. Our results show that this novel plasmid shuttle vector can be used for transformation of animal isolate *C. pneumoniae* LPCoLN as well as human cardiovascular isolate *C. pneumoniae* CV-6. Transformation leads to RSGFP expressing chlamydiae which can be observed using fluorescence microscope without previous staining. Further transformation experiments revealed that *C. felis* can overcome chlamydial plasmid tropism when pRSGFPCAT-Cpn was used. These results led to a hypothesis that horizontal gene transfer among chlamydiae using plasmids might be possible and relevant to public health.

Now, this new plasmid shuttle vector is ready to use for further *C. pneumoniae* research. This novel system can shed light on yet unknown findings about chlamydial pathogenesis and tissue tropism. Newly gained knowledge about this unique pathogen which can be used to identify new drug targets can lead to the development of novel therapeutic approaches or prophylactic vaccines against chlamydial

infections. Finally, these achievements will facilitate the management of chlamydial infection in daily clinical routine.

8 References

1. Bertani G. Lysogeny at Mid-Twentieth Century: P1, P2, and Other Experimental Systems. J Bacteriol. 2004 Feb 1;186(3):595–600.

2. Bayramova F, Jacquier N, Greub G. Insight in the biology of Chlamydia-related bacteria. Microbes Infect. 2018 Aug 1;20(7):432–40.

3. Elwell C, Mirrashidi K, Engel J. Chlamydia cell biology and pathogenesis. Nat Rev Microbiol. 2016 Jun;14(6):385–400.

4. AbdelRahman YM, Belland RJ. The chlamydial developmental cycle: Figure 1. FEMS Microbiol Rev. 2005 Nov;29(5):949–59.

5. Tan M, Bavoil P, editors. Intracellular Pathogens I: Chlamydiales. 1st ed. Washington, DC: ASM Press; 2012. 406 p.

6. Omsland A, Sixt BS, Horn M, Hackstadt T. Chlamydial metabolism revisited: interspecies metabolic variability and developmental stage-specific physiologic activities. FEMS Microbiol Rev. 2014 Jul;38(4):779–801.

7. Saka HA, Thompson JW, Chen Y-S, Kumar Y, Dubois LG, Moseley MA, et al. Quantitative proteomics reveals metabolic and pathogenic properties of Chlamydia trachomatis developmental forms. Mol Microbiol. 2011 Dec;82(5):1185–203.

8. Wolf K, Fischer E, Hackstadt T. Ultrastructural analysis of developmental events in Chlamydia pneumoniae-infected cells. Infect Immun. 2000 Apr;68(4):2379–85.

9. Hackstadt T, Fischer ER, Scidmore MA, Rockey DD, Heinzen RA. Origins and functions of the chlamydial inclusion. Trends Microbiol. 1997 Jul;5(7):288–93.

10. Heuer D, Rejman Lipinski A, Machuy N, Karlas A, Wehrens A, Siedler F, et al. Chlamydia causes fragmentation of the Golgi compartment to ensure reproduction. Nature. 2009 Feb 5;457(7230):731–5.

11. Panzetta ME, Valdivia RH, Saka HA. Chlamydia Persistence: A Survival Strategy to Evade Antimicrobial Effects in-vitro and in-vivo. Front Microbiol. 2018;9:3101.

12. Gieffers J, Rupp J, Gebert A, Solbach W, Klinger M. First-choice antibiotics at subinhibitory concentrations induce persistence of Chlamydia pneumoniae. Antimicrob Agents Chemother. 2004 Apr;48(4):1402–5.

13. Skilton RJ, Cutcliffe LT, Barlow D, Wang Y, Salim O, Lambden PR, et al. Penicillin Induced Persistence in Chlamydia trachomatis: High Quality Time Lapse Video Analysis of the Developmental Cycle. Kelly KA, editor. PLoS ONE. 2009 Nov 6;4(11):e7723.

14. Beatty WL, Morrison RP, Byrne GI. Persistent chlamydiae: from cell culture to a paradigm for chlamydial pathogenesis. Microbiol Rev. 1994 Dec;58(4):686–99.

15. Huston WM, Theodoropoulos C, Mathews SA, Timms P. Chlamydia trachomatis responds to heat shock, penicillin induced persistence, and IFN-gamma persistence by altering levels of the extracytoplasmic stress response protease HtrA. BMC Microbiol. 2008 Nov 6;8:190.

16. Pettengill MA, Lam VW, Ojcius DM. The Danger Signal Adenosine Induces Persistence of Chlamydial Infection through Stimulation of A2b Receptors. PLOS ONE. 2009 Dec 14;4(12):e8299.

17. Harper A, Pogson CI, Jones ML, Pearce JH. Chlamydial development is adversely affected by minor changes in amino acid supply, blood plasma amino acid levels, and glucose deprivation. Infect Immun. 2000 Mar;68(3):1457–64.

18. Wiedeman JA, Kaul R, Heuer LS, Thao NN, Pinkerton KE, Wenman WM. Tobacco smoke induces a persistent, but recoverable state in Chlamydia pneumoniae infection of human endothelial cells. Microb Pathog. 2005 Dec;39(5–6):197–204.

19. Hsia R, Ohayon H, Gounon P, Dautry-Varsat A, Bavoil PM. Phage infection of the obligate intracellular bacterium, Chlamydia psittaci strain guinea pig inclusion conjunctivitis. Microbes Infect. 2000 Jun;2(7):761–72.

20. Vanover J, Kintner J, Whittimore J, Schoborg RV. Interaction of herpes simplex virus type 2 (HSV-2) glycoprotein D with the host cell surface is sufficient to induce Chlamydia trachomatis persistence. Microbiol Read Engl. 2010 May;156(Pt 5):1294–302.

21. Prusty BK, Böhme L, Bergmann B, Siegl C, Krause E, Mehlitz A, et al. Imbalanced oxidative stress causes chlamydial persistence during non-productive human herpes virus co-infection. PloS One. 2012;7(10):e47427.

22. Schoborg RV, Borel N. Porcine epidemic diarrhea virus (PEDV) co-infection induced chlamydial persistence/stress does not require viral replication. Front Cell Infect Microbiol. 2014;4:20.

23. Borel N, Summersgill JT, Mukhopadhyay S, Miller RD, Ramirez JA, Pospischil A. Evidence for persistent Chlamydia pneumoniae infection of human coronary atheromas. Atherosclerosis. 2008 Jul;199(1):154–61.

24. Airenne S, Surcel H-M, Alakärppä H, Laitinen K, Paavonen J, Saikku P, et al. Chlamydia pneumoniae Infection in Human Monocytes. Infect Immun. 1999 Mar;67(3):1445–9.

25. Pospischil A, Borel N, Chowdhury EH, Guscetti F. Aberrant chlamydial developmental forms in the gastrointestinal tract of pigs spontaneously and experimentally infected with Chlamydia suis. Vet Microbiol. 2009 Mar 16;135(1–2):147–56.

26. Rank RG, Whittimore J, Bowlin AK, Wyrick PB. In vivo ultrastructural analysis of the intimate relationship between polymorphonuclear leukocytes and the chlamydial developmental cycle. Infect Immun. 2011 Aug;79(8):3291–301.

27. Phillips Campbell R, Kintner J, Whittimore J, Schoborg RV. Chlamydia muridarum enters a viable but non-infectious state in amoxicillin-treated BALB/c mice. Microbes Infect. 2012 Nov;14(13):1177–85.

28. Lewis ME, Belland RJ, AbdelRahman YM, Beatty WL, Aiyar AA, Zea AH, et al. Morphologic and molecular evaluation of Chlamydia trachomatis growth in human endocervix reveals distinct growth patterns. Front Cell Infect Microbiol. 2014;4:71.

29. Bachmann NL, Polkinghorne A, Timms P. Chlamydia genomics: providing novel insights into chlamydial biology. Trends Microbiol. 2014 Aug;22(8):464–72.

30. Grayston JT, Kuo C-C, Campbell LA, Wang S-P. Chlamydia pneumoniae sp. nov. for Chlamydia sp. Strain TWAR. Int J Syst Bacteriol. 1989 Jan 1;39(1):88–90.

31. Taxonomy browser (Chlamydia) [Internet]. [cited 2020 Jul 10]. Available from: https://www.ncbi.nlm.nih.gov/Taxonomy/Browser/wwwtax.cgi?id=810

32. Sachse K, Bavoil PM, Kaltenboeck B, Stephens RS, Kuo C-C, Rosselló-Móra R, et al. Emendation of the family Chlamydiaceae: proposal of a single genus, Chlamydia, to include all currently recognized species. Syst Appl Microbiol. 2015 Mar;38(2):99–103.

33. Sachse K, Laroucau K, Riege K, Wehner S, Dilcher M, Creasy HH, et al. Evidence for the existence of two new members of the family Chlamydiaceae and proposal of Chlamydia avium sp. nov. and Chlamydia gallinacea sp. nov. Syst Appl Microbiol. 2014 Mar;37(2):79–88.

34. Everett KDE, Bush RM, Andersen AA. Emended description of the order Chlamydiales, proposal of Parachlamydiaceae fam. nov. and Simkaniaceae fam. nov., each containing one monotypic genus, revised taxonomy of the family Chlamydiaceae, including a new genus and five new species, and standards for the identification of organisms. Int J Syst Evol Microbiol. 1999;49(2):415–40.

35. Fukushi H, Hirai K. Proposal of Chlamydia pecorum sp. nov. for Chlamydia strains derived from ruminants. Int J Syst Bacteriol. 1992 Apr;42(2):306–8.

36. Vorimore F, Hsia R, Huot-Creasy H, Bastian S, Deruyter L, Passet A, et al. Isolation of a New Chlamydia species from the Feral Sacred Ibis (Threskiornis aethiopicus): Chlamydia ibidis. PLOS ONE. 2013 Sep 20;8(9):e74823.

37. Laroucau K, Vorimore F, Aaziz R, Solmonson L, Hsia RC, Bavoil PM, et al. Chlamydia buteonis, a new Chlamydia species isolated from a red-shouldered hawk. Syst Appl Microbiol. 2019 Sep;42(5):125997.

38. Parte AC. LPSN—list of prokaryotic names with standing in nomenclature. Nucleic Acids Res. 2014 Jan 1;42(Database issue):D613–6.

39. All names cited in the List of Prokaryotic names with Standing in Nomenclature: List A-C [Internet]. [cited 2019 Oct 25]. Available from: http://www.bacterio.net/-allnamesac.html#r

40. Stephens RS, Myers G, Eppinger M, Bavoil PM. Divergence without difference: phylogenetics and taxonomy of Chlamydia resolved. FEMS Immunol Med Microbiol. 2009 Mar 1;55(2):115–9.

41. Schachter J, Stephens RS, Timms P, Kuo C, Bavoil PM, Birkelund S, et al. Radical changes to chlamydial taxonomy are not necessary just yet. Int J Syst Evol Microbiol. 2001 Jan;51(Pt 1):249; author reply 251-253.

42. Campbell LA, Kuo C. Chlamydia pneumoniae — an infectious risk factor for atherosclerosis? Nat Rev Microbiol. 2004 Jan;2(1):23–32.

43. Roulis E, Polkinghorne A, Timms P. Chlamydia pneumoniae: modern insights into an ancient pathogen. Trends Microbiol. 2013 Mar;21(3):120–8.

44. Kuo CC, Chen HH, Wang SP, Grayston JT. Identification of a new group of Chlamydia psittaci strains called TWAR. J Clin Microbiol. 1986 Dec;24(6):1034–7.

45. Grayston JT, Kuo C, Wang S, Altman J. A New Chlamydia psittaci Strain, TWAR, Isolated in Acute Respiratory Tract Infections. N Engl J Med. 1986 Jul 17;315(3):161–8.

46. Sixt BS, Valdivia RH. Molecular Genetic Analysis of *Chlamydia* Species. Annu Rev Microbiol. 2016 Sep 8;70(1):179–98.

47. Bush RM, Everett KD. Molecular evolution of the Chlamydiaceae. Int J Syst Evol Microbiol. 2001;51(1):203–20.

48. Kalman S, Mitchell W, Marathe R, Lammel C, Fan J, Hyman RW, et al. Comparative genomes of Chlamydia pneumoniae and C. trachomatis. Nat Genet. 1999 Apr;21(4):385–9.

49. Weinmaier T, Hoser J, Eck S, Kaufhold I, Shima K, Strom TM, et al. Genomic factors related to tissue tropism in Chlamydia pneumoniae infection. BMC Genomics. 2015 Apr 7;16(1):268.

50. Rattei T, Ott S, Gutacker M, Rupp J, Maass M, Schreiber S, et al. Genetic diversity of the obligate intracellular bacterium Chlamydophila pneumoniae by genome-wide analysis of single nucleotide polymorphisms: evidence for highly clonal population structure. BMC Genomics. 2007 Oct 4;8:355.

51. Gieffers J, Durling L, Ouellette SP, Rupp J, Maass M, Byrne GI, et al. Genotypic Differences in the Chlamydia pneumoniae tyrP Locus Related to Vascular Tropism and Pathogenicity. J Infect Dis. 2003 Oct 15;188(8):1085–93.

52. Myers GSA, Mathews SA, Eppinger M, Mitchell C, O'Brien KK, White OR, et al. Evidence that Human Chlamydia pneumoniae Was Zoonotically Acquired. J Bacteriol. 2009 Dec 1;191(23):7225–33.

53. Wills JM, Watson G, Lusher M, Mair TS, Wood D, Richmond SJ. Characterization of Chlamydia psittaci isolated from a horse. Vet Microbiol. 1990 Jul 1;24(1):11–9.

54. Kutlin A, Roblin PM, Kumar S, Kohlhoff S, Bodetti T, Timms P, et al. Molecular characterization of Chlamydophila pneumoniae isolates from Western barred bandicoots. J Med Microbiol. 2007;56(3):407–17.

55. Kauppinen M, Saikku P. Pneumonia due to Chlamydia pneumoniae: prevalence, clinical features, diagnosis, and treatment. Clin Infect Dis Off Publ Infect Dis Soc Am. 1995 Dec;21 Suppl 3:S244-252.

56. Cunha BA. The atypical pneumonias: clinical diagnosis and importance. Clin Microbiol Infect Off Publ Eur Soc Clin Microbiol Infect Dis. 2006 May;12 Suppl 3:12–24.

57. Sharma L, Losier A, Tolbert T, Dela Cruz CS, Marion CR. Atypical Pneumonia: Updates on Legionella, Chlamydophila, and Mycoplasma Pneumonia. Clin Chest Med. 2017 Mar;38(1):45–58.

58. Hahn DL, Schure A, Patel K, Childs T, Drizik E, Webley W. Chlamydia pneumoniae-Specific IgE Is Prevalent in Asthma and Is Associated with Disease Severity. PLoS ONE [Internet]. 2012 Apr 24 [cited 2019 Nov 5];7(4). Available from: https://www.ncbi.nlm.nih.gov/pmc/articles/PMC3335830/

59. Zaitsu M. The Development of Asthma In Wheezing Infants with Chlamydia pneumoniae Infection. J Asthma. 2007 Jan 1;44(7):565–8.

60. Webley WC, Hahn DL. Infection-mediated asthma: etiology, mechanisms and treatment options, with focus on Chlamydia pneumoniae and macrolides. Respir Res. 2017 19;18(1):98.

61. Muro S, Tabara Y, Matsumoto H, Setoh K, Kawaguchi T, Takahashi M, et al. Relationship Among Chlamydia and Mycoplasma Pneumoniae Seropositivity, IKZF1 Genotype and Chronic Obstructive Pulmonary Disease in A General Japanese Population. Medicine (Baltimore) [Internet]. 2016 Apr 18 [cited 2019 Nov 5];95(15). Available from: https://www.ncbi.nlm.nih.gov/pmc/articles/PMC4839845/

62. Grayston JT. Background and current knowledge of Chlamydia pneumoniae and atherosclerosis. J Infect Dis. 2000 Jun;181 Suppl 3:S402-410.

63. Deniset JF, Cheung PKM, Dibrov E, Lee K, Steigerwald S, Pierce GN. Chlamydophila pneumoniae Infection Leads to Smooth Muscle Cell Proliferation and Thickening in the Coronary Artery without Contributions from a Host Immune Response. Am J Pathol. 2010 Feb;176(2):1028–37.

64. Hasan ZN. Association of Chlamydia pneumoniae serology and ischemic stroke. South Med J. 2011 May;104(5):319–21.

65. Maass M, Bartels C, Engel PM, Mamat U, Sievers H-H. Endovascular Presence of Viable Chlamydia pneumoniaeIs a Common Phenomenon in Coronary Artery Disease 11This study was supported in part by the Research

Commission of the Medical University of Lübeck (8/96) and the Deutsche Forschungsgemeinschaft (SFB 367/B2), Bonn, Germany. J Am Coll Cardiol. 1998 Mar 15;31(4):827–32.

66. Saikku P, Mattila K, Nieminen MS, Huttunen JK, Leinonen M, Ekman M-R, et al. SEROLOGICAL EVIDENCE OF AN ASSOCIATION OF A NOVEL CHLAMYDIA, TWAR, WITH CHRONIC CORONARY HEART DISEASE AND ACUTE MYOCARDIAL INFARCTION. The Lancet. 1988 Oct 29;332(8618):983–6.

67. Filardo S, Di Pietro M, Farcomeni A, Schiavoni G, Sessa R. Chlamydia pneumoniae-Mediated Inflammation in Atherosclerosis: A Meta-Analysis. Mediators Inflamm [Internet]. 2015 [cited 2019 Nov 7];2015. Available from: https://www.ncbi.nlm.nih.gov/pmc/articles/PMC4546765/

68. Taylor-Robinson D, Thomas BJ. Chlamydia pneumoniae in Atherosclerotic Tissue. J Infect Dis. 2000 Jun 1;181(Supplement_3):S437–40.

69. Witte L, Droemann D, Dalhoff K, Rupp J. Chlamydia pneumoniae is frequently detected in the blood after acute lung infection. Eur Respir J. 2011 Mar 1;37(3):712–4.

70. Gieffers Jens, Füllgraf Henriette, Jahn Jürgen, Klinger Matthias, Dalhoff Klaus, Katus Hugo A., et al. Chlamydia pneumoniae Infection in Circulating Human Monocytes Is Refractory to Antibiotic Treatment. Circulation. 2001 Jan 23;103(3):351–6.

71. Porritt RA, Crother TR. Chlamydia pneumoniae Infection and Inflammatory Diseases. Forum Immunopathol Dis Ther. 2016;7(3–4):237–54.

72. Azenabor AA, Yang S, Job G, Adedokun OO. Elicitation of reactive oxygen species in Chlamydia pneumoniae-stimulated macrophages: a Ca2+-dependent process involving simultaneous activation of NADPH oxidase and cytochrome oxidase genes. Med Microbiol Immunol (Berl). 2005 Jan;194(1–2):91–103.

73. Kälvegren H, Bylin H, Leanderson P, Richter A, Grenegård M, Bengtsson T. Chlamydia pneumoniae induces nitric oxide synthase and lipoxygenase-dependent production of reactive oxygen species in platelets. Effects on oxidation of low density lipoproteins. Thromb Haemost. 2005 Aug;94(2):327–35.

74. Chen S, Shimada K, Zhang W, Huang G, Crother TR, Arditi M. IL-17A is proatherogenic in high-fat diet-induced and Chlamydia pneumoniae-infection accelerated atherosclerosis in mice. J Immunol Baltim Md 1950. 2010 Nov 1;185(9):5619–27.

75. Dreses-Werringloer U, Bhuiyan M, Zhao Y, Gérard HC, Whittum-Hudson JA, Hudson AP. Initial characterization of Chlamydophila (Chlamydia) pneumoniae cultured from the late-onset Alzheimer brain. Int J Med Microbiol IJMM. 2009 Mar;299(3):187–201.

76. Shima K, Kuhlenbäumer G, Rupp J. Chlamydia pneumoniae infection and Alzheimer's disease: a connection to remember? Med Microbiol Immunol (Berl). 2010 Nov;199(4):283–9.

77. Wang C, Gao D, Kaltenboeck B. Acute Chlamydia pneumoniae reinfection accelerates the development of insulin resistance and diabetes in obese C57BL/6 mice. J Infect Dis. 2009 Jul 15;200(2):279–87.

78. Ayaşlioğlu E, Düzgün N, Erkek E, Inal A. Evidence of chronic Chlamydia pneumoniae infection in patients with Behçet's disease. Scand J Infect Dis. 2004;36(6–7):428–30.

79. Abdulkarim AS, Petrovic LM, Kim WR, Angulo P, Lloyd RV, Lindor KD. Primary biliary cirrhosis: an infectious disease caused by Chlamydia pneumoniae? J Hepatol. 2004 Mar;40(3):380–4.

80. Zhan P, Suo L, Qian Q, Shen X, Qiu L-X, Yu L, et al. Chlamydia pneumoniae infection and lung cancer risk: a meta-analysis. Eur J Cancer Oxf Engl 1990. 2011 Mar;47(5):742–7.

81. Hua-Feng X, Yue-Ming W, Hong L, Junyi D. A meta-analysis of the association between Chlamydia pneumoniae infection and lung cancer risk. Indian J Cancer. 2015 Dec;52 Suppl 2:e112-115.

82. Carter JD, Hudson AP. The evolving story of Chlamydia-induced reactive arthritis. Curr Opin Rheumatol. 2010 Jul;22(4):424–30.

83. Carter JD, Hudson AP. Recent advances and future directions in understanding and treating Chlamydia-induced reactive arthritis. Expert Rev Clin Immunol. 2017 Mar;13(3):197–206.

84. Tam JE, Davis CH, Wyrick PB. Expression of recombinant DNA introduced into Chlamydia trachomatis by electroporation. Can J Microbiol. 1994 Jul;40(7):583–91.

85. Binet R, Maurelli AT. Transformation and isolation of allelic exchange mutants of Chlamydia psittaci using recombinant DNA introduced by electroporation. Proc Natl Acad Sci U S A. 2009 Jan 6;106(1):292–7.

86. Wang Y, Kahane S, Cutcliffe LT, Skilton RJ, Lambden PR, Clarke IN. Development of a Transformation System for Chlamydia trachomatis: Restoration of Glycogen Biosynthesis by Acquisition of a Plasmid Shuttle Vector. Valdivia RH, editor. PLoS Pathog. 2011 Sep 22;7(9):e1002258.

87. Madigan MT, Martinko JM. Brock Mikrobiologie. 11. Auflage. 11., aktualisierte Auflage 2009. München: Pearson Studium; 2008. 1248 p.

88. Urry LA, Cain ML, Wasserman SA, Minorsky PV, Reece JB. Campbell Biologie. Mit eLearning-Zugang "MyLab | Biologie." 11., aktualisierte. Pearson Studium; 2019. 1824 p.

89. Biotechnologie - Thieman, William J.; Palladino, Michael A. - 9783827372369 - Biology - Biotechnology (101) [Internet]. [cited 2019 Nov 17]. Available from:

https://www.pearson.ch/HigherEducation/PearsonStudium/EAN/9783827372369/Biotechnologie

90. Comanducci M, Ricci S, Cevenini R, Ratti G. Diversity of the Chlamydia trachomatis common plasmid in biovars with different pathogenicity. Plasmid. 1990 Mar 1;23(2):149–54.

91. Thomas NS, Lusher M, Storey CC, Clarke IN. Plasmid diversity in Chlamydia. Microbiol Read Engl. 1997 Jun;143 (Pt 6):1847–54.

92. Li Z, Chen D, Zhong Y, Wang S, Zhong G. The Chlamydial Plasmid-Encoded Protein pgp3 Is Secreted into the Cytosol of Chlamydia-Infected Cells. Infect Immun. 2008 Aug 1;76(8):3415–28.

93. Ferreira R, Borges V, Nunes A, Borrego MJ, Gomes JP. Assessment of the load and transcriptional dynamics of Chlamydia trachomatis plasmid according to strains' tissue tropism. Microbiol Res. 2013 Jul 19;168(6):333–9.

94. Song L, Carlson JH, Whitmire WM, Kari L, Virtaneva K, Sturdevant DE, et al. Chlamydia trachomatis Plasmid-Encoded Pgp4 Is a Transcriptional Regulator of Virulence-Associated Genes. Morrison RP, editor. Infect Immun. 2013 Mar;81(3):636–44.

95. Song L, Carlson JH, Zhou B, Virtaneva K, Whitmire WM, Sturdevant GL, et al. Plasmid-mediated transformation tropism of chlamydial biovars. Pathog Dis. 2014 Mar 1;70(2):189–93.

96. Zhong G. Chlamydial Plasmid-Dependent Pathogenicity. Trends Microbiol. 2017 Feb;25(2):141–52.

97. Wang Y, Cutcliffe LT, Skilton RJ, Ramsey KH, Thomson NR, Clarke IN. The genetic basis of plasmid tropism between *Chlamydia trachomatis* and *Chlamydia muridarum*. Pathog Dis. 2014 Oct;72(1):19–23.

98. Di Francesco A, Donati M, Salvatore D, Cevenini R, Di Paolo M, Baldelli R. Chlamydophila felis: plasmid detection in Italian isolates. New Microbiol. 2010 Apr;33(2):163–6.

99. Jelocnik M, Bachmann NL, Kaltenboeck B, Waugh C, Woolford L, Speight KN, et al. Genetic diversity in the plasticity zone and the presence of the chlamydial plasmid differentiates Chlamydia pecorum strains from pigs, sheep, cattle, and koalas. BMC Genomics [Internet]. 2015 Dec [cited 2018 Sep 11];16(1). Available from: http://www.biomedcentral.com/1471-2164/16/893

100. Harley R, Day S, Di Rocco C, Helps C. The Chlamydophila felis plasmid is highly conserved. Vet Microbiol. 2010 Nov 20;146(1–2):172–4.

101. Frazer LC, Darville T, Chandra-Kuntal K, Andrews CW, Zurenski M, Mintus M, et al. Plasmid-Cured Chlamydia caviae Activates TLR2-Dependent Signaling and Retains Virulence in the Guinea Pig Model of Genital Tract Infection. Kelly KA, editor. PLoS ONE. 2012 Jan 24;7(1):e30747.

102. O'Connell CM. A plasmid-cured Chlamydia muridarum strain displays altered plaque morphology and reduced infectivity in cell culture. Microbiology. 2006 Jun 1;152(6):1601–7.

103. Gong S, Yang Z, Lei L, Shen L, Zhong G. Characterization of Chlamydia trachomatis Plasmid-Encoded Open Reading Frames. J Bacteriol. 2013 Sep 1;195(17):3819–26.

104. Wang Y, Kahane S, Cutcliffe LT, Skilton RJ, Lambden PR, Persson K, et al. Genetic transformation of a clinical (genital tract), plasmid-free isolate of Chlamydia trachomatis: engineering the plasmid as a cloning vector. PloS One. 2013;8(3):e59195.

105. Agaisse H, Derré I. A C. trachomatis Cloning Vector and the Generation of C. trachomatis Strains Expressing Fluorescent Proteins under the Control of a C. trachomatis Promoter. Rudel T, editor. PLoS ONE. 2013 Feb 18;8(2):e57090.

106. Xu S, Battaglia L, Bao X, Fan H. Chloramphenicol acetyltransferase as a selection marker for chlamydial transformation. BMC Res Notes. 2013;6(1):377.

107. WHO | WHO guidelines for the treatment of *Chlamydia trachomatis* [Internet]. WHO. [cited 2019 Oct 14]. Available from: http://www.who.int/reproductivehealth/publications/rtis/chlamydia-treatment-guidelines/en/

108. Mitchell CM, Hovis KM, Bavoil PM, Myers GS, Carrasco JA, Timms P. Comparison of koala LPCoLN and human strains of Chlamydia pneumoniae highlights extended genetic diversity in the species. BMC Genomics. 2010 Jul 21;11(1):442.

109. Roulis E, Bachmann N, Polkinghorne A, Hammerschlag M, Kohlhoff S, Timms P. Draft Genome and Plasmid Sequences of Chlamydia pneumoniae Strain B21 from an Australian Endangered Marsupial, the Western Barred Bandicoot. Genome Announc. 2014 Feb 27;2(1):e01223-13.

110. Azuma Y, Hirakawa H, Yamashita A, Cai Y, Rahman MA, Suzuki H, et al. Genome Sequence of the Cat Pathogen, Chlamydophila felis. DNA Res. 2006 Jan 1;13(1):15–23.

111. Lusher M, Storey CC, Richmond SJ. Plasmid Diversity within the Genus Chlamydia. Microbiology. 1989 May 1;135(5):1145–51.

112. Wons J, Meiller R, Bergua A, Bogdan C, Geißdörfer W. Follicular Conjunctivitis due to Chlamydia felis-Case Report, Review of the Literature and Improved Molecular Diagnostics. Front Med. 2017;4:105.

113. Ochman H, Lawrence JG, Groisman EA. Lateral gene transfer and the nature of bacterial innovation. Nature. 2000 May;405(6784):299–304.

114. Soucy SM, Huang J, Gogarten JP. Horizontal gene transfer: building the web of life. Nat Rev Genet. 2015 Aug;16(8):472–82.

115. Suchland RJ, Sandoz KM, Jeffrey BM, Stamm WE, Rockey DD. Horizontal Transfer of Tetracycline Resistance among Chlamydia spp. In Vitro. Antimicrob Agents Chemother. 2009 Nov;53(11):4604–11.

116. DeMars R, Weinfurter J, Guex E, Lin J, Potucek Y. Lateral Gene Transfer In Vitro in the Intracellular Pathogen Chlamydia trachomatis. J Bacteriol. 2007 Feb 1;189(3):991–1003.

117. Carvelli A, Iacoponi F, Scaramozzino P. A Cross-Sectional Survey to Estimate the Cat Population and Ownership Profiles in a Semirural Area of Central Italy [Internet]. BioMed Research International. 2016 [cited 2019 Oct 22]. Available from: https://www.hindawi.com/journals/bmri/2016/3796872/

118. Murray JK, Gruffydd-Jones TJ, Roberts MA, Browne WJ. Assessing changes in the UK pet cat and dog populations: numbers and household ownership. Vet Rec. 2015 Sep 12;177(10):259–259.

119. World Health Organization. WHO guidelines on use of medically important antimicrobials in food-producing animals. 2017.

120. Vromman F, Laverrière M, Perrinet S, Dufour A, Subtil A. Quantitative Monitoring of the Chlamydia trachomatis Developmental Cycle Using GFP-Expressing Bacteria, Microscopy and Flow Cytometry. PLOS ONE. 2014 Jun 9;9(6):e99197.

121. Campbell J, Huang Y, Liu Y, Schenken R, Arulanandam B, Zhong G. Bioluminescence Imaging of Chlamydia muridarum Ascending Infection in Mice. PLOS ONE. 2014 Jul 1;9(7):e101634.

122. Perez-Pinera P, Menendez-Gonzalez M, Vega JA. Deletion of DNA sequences of using a polymerase chain reaction based approach. Electron J Biotechnol. 2006 Oct 15;9(5):0–0.

123. Bryksin A, Matsumura I. Overlap extension PCR cloning: a simple and reliable way to create recombinant plasmids. BioTechniques. 2010 Jun;48(6):463–5.

124. Kari L, Goheen MM, Randall LB, Taylor LD, Carlson JH, Whitmire WM, et al. Generation of targeted Chlamydia trachomatis null mutants. Proc Natl Acad Sci. 2011 Apr 26;108(17):7189–93.

125. Johnson CM, Fisher DJ. Site-Specific, Insertional Inactivation of incA in Chlamydia trachomatis Using a Group II Intron. PLOS ONE. 2013 Dec 31;8(12):e83989.

126. Mueller KE, Wolf K, Fields KA. Gene Deletion by Fluorescence-Reported Allelic Exchange Mutagenesis in *Chlamydia trachomatis*. mBio [Internet]. 2016 Mar 2 [cited 2018 Sep 11];7(1). Available from: http://mbio.asm.org/lookup/doi/10.1128/mBio.01817-15

127. Abdelsamed H, Peters J, Byrne GI. Genetic variation in Chlamydia trachomatis and their hosts: impact on disease severity and tissue tropism. Future Microbiol. 2013 Sep;8(9):1129–46.

128. Cochrane M, Walker P, Gibbs H, Timms P. Multiple genotypes of Chlamydia pneumoniae identified in human carotid plaque. Microbiol Read Engl. 2005 Jul;151(Pt 7):2285–90.

129. Gieffers J, Solbach W, Maass M. In Vitro Susceptibilities of Chlamydia pneumoniae Strains Recovered from Atherosclerotic Coronary Arteries. Antimicrob Agents Chemother. 1998 Oct;42(10):2762.

130. Dwyer RS, Treharne JD, Jones BR, Herring J. Chlamydial infection. Results of micro-immunofluorescence tests for the detection of type-specific antibody in certain chlamydial infections. Br J Vener Dis. 1972 Dec;48(6):452–9.

131. Sachse K, Hotzel H, Slickers P, Ellinger T, Ehricht R. DNA microarray-based detection and identification of Chlamydia and Chlamydophila spp. Mol Cell Probes. 2005 Feb 1;19(1):41–50.

132. Baym M, Kryazhimskiy S, Lieberman TD, Chung H, Desai MM, Kishony R. Inexpensive Multiplexed Library Preparation for Megabase-Sized Genomes. PLOS ONE. 2015 May 22;10(5):e0128036.

133. Babraham Bioinformatics - FastQC A Quality Control tool for High Throughput Sequence Data [Internet]. [cited 2019 Sep 19]. Available from: http://www.bioinformatics.babraham.ac.uk/projects/fastqc/

134. Bolger AM, Lohse M, Usadel B. Trimmomatic: a flexible trimmer for Illumina sequence data. Bioinformatics. 2014 Aug 1;30(15):2114–20.

135. Li H, Durbin R. Fast and accurate short read alignment with Burrows–Wheeler transform. Bioinformatics. 2009 Jul 15;25(14):1754–60.

136. Li H, Handsaker B, Wysoker A, Fennell T, Ruan J, Homer N, et al. The Sequence Alignment/Map format and SAMtools. Bioinformatics. 2009 Aug 15;25(16):2078–9.

137. Picard Tools - By Broad Institute [Internet]. [cited 2019 Sep 19]. Available from: https://broadinstitute.github.io/picard/

138. Garrison E, Marth G. Haplotype-based variant detection from short-read sequencing. ArXiv12073907 Q-Bio [Internet]. 2012 Jul 17 [cited 2019 Sep 19]; Available from: http://arxiv.org/abs/1207.3907

139. BBMap [Internet]. SourceForge. [cited 2019 Sep 19]. Available from: https://sourceforge.net/projects/bbmap/

140. Nurk S, Bankevich A, Antipov D, Gurevich A, Korobeynikov A, Lapidus A, et al. Assembling Genomes and Mini-metagenomes from Highly Chimeric Reads. In: Deng M, Jiang R, Sun F, Zhang X, editors. Research in Computational Molecular Biology. Springer Berlin Heidelberg; 2013. p. 158–70. (Lecture Notes in Computer Science).

141. Gurevich A, Saveliev V, Vyahhi N, Tesler G. QUAST: quality assessment tool for genome assemblies. Bioinformatics. 2013 Apr 15;29(8):1072–5.

142. Altschul SF, Gish W, Miller W, Myers EW, Lipman DJ. Basic local alignment search tool. J Mol Biol. 1990 Oct 5;215(3):403–10.

143. Huson DH, Beier S, Flade I, Górska A, El-Hadidi M, Mitra S, et al. MEGAN Community Edition - Interactive Exploration and Analysis of Large-Scale Microbiome Sequencing Data. PLOS Comput Biol. 2016 Jun 21;12(6):e1004957.

9 List of figures

10 List of tables

11 Appendix

11.1 Publication

Kensuke Shima, **Maximilian Wanker**, Rachel J. Skilton, Lesley T. Cutcliffe, Christiane Schnee, Thomas A. Kohl, Stefan Niemann, Javier Geijo, Matthias Klinger, Peter Timms, Thomas Rattei, Konrad Sachse, Ian N. Clarke, Jan Rupp: *"The Genetic Transformation of Chlamydia pneumoniae."* *mSphere* 3, no. 5 (10 2018). https://doi.org/10.1128/mSphere.00412-18.

11.2 Congress

Maximilian Wanker, Kensuke Shima, Matthias Klinger, Jan Rupp: *Genetische Modifikation von Chlamydien.* „Uni im Dialog“, University of Lübeck (28.06.2017 in Lübeck, Germany), Poster.

Nis Phillip Schmidt, **Maximilian Wanker**, Nadja Käding, Kensuke Shima, Jan Rupp: *Anti-metabolic effects of the first-choice antimicrobials against C. trachomatis.* Annual Meeting of the German Society of Infectious Diseases (DGI) and the German Center for Infection Research (DZIF) (28.-30.09.2017 in Hamburg, Germany), Poster

Maximilian Wanker, Kensuke Shima, Rachel J. Skilton, Lesley T. Cutcliffe, Christiane Schnee, Thomas A. Kohl, Stefan Niemann, Javier Geijo, Matthias Klinger, Peter Timms, Thomas Rattei, Konrad Sachse, Ian N. Clarke, Jan Rupp: *The genetic transformation of Chlamydia pneumoniae*. 6thTranslational DZIF-School (7.-9.11.2018 in Lübeck, Germany), Poster

Maximilian Wanker, Kensuke Shima, Rachel J. Skilton, Lesley T. Cutcliffe, Christiane Schnee, Thomas A. Kohl, Stefan Niemann, Javier Geijo, Matthias Klinger, Peter Timms, Thomas Rattei, Konrad Sachse, Ian N. Clarke, Jan Rupp: *The genetic transformation of Chlamydia pneumoniae*. „Tag der Deutschen Zentren für Gesundheitsforschung in Lübeck“ (30.11.2018 in Lübeck, Germany), Poster

11.3 Supplement

11.3.1 Bacterial strains

All bacteria from table 10 except for *C. pneumoniae* N16 were used for transformation experiments which are described in this thesis. The extrachromosomal plasmid pCpnE1 of *C. pneumoniae* N16 (7,368 bp; GenBank accession no. X82078.1) was used as backbone for the construction of the pRSGFPCAT-Cpn plasmid shuttle vector and was provided by Prof. Ian Clarke (University of Southampton, Southampton, United Kingdom). For the sake of completeness *C. pneumoniae* N16 is listed in table 10.

C. pneumoniae LPCoLN is an animal isolated strain. It was provided by Prof. Peter Timms (University of Sunshine Coast, Maroochydore, Australia) (52).

The human isolate *C. pneumoniae* CV-6 is a cardiovascular strain and was collected by Matthias Maass M.D. in 1998 (University of Lübeck, Lübeck, Germany) (65,129).

Both *C. felis* Not identified (N.I.) and Cello were part of the bacterial collection of Prof. Ian Clarke (University of Southampton, Southampton, United Kingdom).

The human isolate *C. trachomatis* L2 (25667R) was offered by Luis M. De La Maza M.D. (University of California, Irvine, CA, USA).

The remaining animal isolated *Chlamydia spp.*: *C. felis* 02DC26 (Cf02-23; Host: Cat), *C. muridarum* MoPn/Nigg (DSM-28544; Host: Mouse), *C. pecorum* 14DC102 (E58, DSM-29919; Host: Cattle*)*, *C. abortus* C18/98 (B577, DSM-27654; Host: Sheep) and *C. caviae* 03DC25 (GPIC, DSM-19441; Host: Guinea pig) were provided by the Friedrich-Loeffler-Institute in Jena, Germany.

DNA microarrays were used for controlling the species identity and for excluding mixed cultures for prospective experiments (40).

For the construction and amplification of the shuttle plasmid vector (e.g. pRSGFP-CAT-Cpn), the conventional *E. coli* strain DH5α and the DNA adenine methylation (dam) and DNA cytosine methylation (dcm) genes deficient strain JM110 was used and ordered from Agilent Technologies, Santa Clara, CA, USA.

11.3.2 Whole genome sequence analyses

Whole genome sequence analyses of *C. felis* N.I. and *C. pneumoniae* CV-6 were performed. Our results show a high similarity of 99.99% between *C. felis* N.I. and

C. felis Fe/C-56. Analyzing the genome of *C. pneumoniae* CV-6 we could show that their genome has a 99.99% conformity with *C. pneumoniae* CV-14.

After DNA isolation Nextera XT DNA Library Prep Kit was used to generate sequencing libraries of extracted chlamydial genome which was performed by using provided manufacturer's instructions or by using lately published protocols for Illumina Nextera Kit (131). Finally, the libraries were sequenced by the NextSeq 500 Sequencing System in a 2- by 151-bp paired-end run. Deconseq v.0.4.3 (132) and the human reference genome GRCh38.p12 were used to eliminate sequence contaminations. FastQC v.0.11.5 (133) was used for quality control checks on raw sequence data. Afterwards data were filtered and trimmed using Trimmomatic (134) which applies minimum quality 28.

Read-based analyses were performed using bwa v.0.7.16a (135). Due to this *C. felis* N.I. was mapped to the reference of *C. felis* Fe/C-56 DNA and *C. pneumoniae* CV-6 was mapped to the reference of *C. pneumoniae* CV-14. Furthermore, sequence reads were mapped to pRSGFPCAT-Cpn.

SAMtools (136) was used to convert alignment data to bam format. In addition, data were sorted and indexed. Picard tools v.2.14.0 (137) was used to eliminate sequence duplicates. FreeBayes v.1.1.0-54 (138) was used for calling variants from data.

Suspected non-polymorphic sequences with a phred quality score less than 20 were removed resulting in filtered vcf files. The bioinformatic tool BBmap v.37.61 (139) was used for mapping statistics of bam files. BCFtools v.16 (136) was used for checking and summarizing variant calling files.

The library of transformed *C. pneumoniae* CV-6 (pRSGFPCAT-Cpn) was compared to a *de novo* library of *C. pneumoniae* CV-6. Therefore, SPAdes v.3.11.1 (140) was used for a *de novo* assembly of the library of *C. pneumoniae* CV-6 with carful parameter and a contig minimum of 500 bp. Results were screened by length and contigs less than 500 bp were removed. The remaining DNA sequences were assessed with Quast v.4.6.3 (141). Resulting data were used for read-based analysis.

SAMtools was used to extracted reads, which were not mapped on their references. Those reads were adjusted to the nt NCBI database, performed by blastn v.2.6.0 (142). Afterwards MEGAN v.6.11.1 (143) was used for taxonomically classification of the results. Due to this, specified weighted last common ancestor (LCA) algorithm, a minimum score of 50 and a Max Expected of 0.1 was set as parameters

and nucleotide accession to the NCBI taxonomy as a mapping file (nucl_acc2tax-Mar2018). No chlamydial DNA sequence were found in investigated classified unmapped reads.

12 Acknowledgments

To end, I would like to thank everyone who supported me in performing and writing this thesis. Without your continuous help and support, this work would not have been possible.

First and foremost, I would like to thank Prof. Dr. Jan Rupp and PD Dr. Kensuke Shima for their permanent support and mentoring during all phases of my graduation. They gave me the opportunity to participate in the scientific world. I cannot neglect that without their support I could not have been that successful. Therefore, I am deeply grateful. Furthermore, I would like to thank all laboratory colleagues for their helpful conversations, constructive feedback and caring support which was essential for my success. In particular, I would like to thank Siegrid Paetzmann from the Department of Infectious Diseases and Microbiology (Lübeck, Germany) for technical assistance. I would also like to thank Prof. Matthias Klinger and his colleagues of the Institute of Anatomy of the University of Lübeck (Lübeck, Germany) who kindly performed the TEM images.

Sincere thanks are given to our laboratory collaborating colleagues of the Department of Molecular and Experimental Mycobacteriology at the Research Center Borstel (Borstel, Germany) for the genome DNA sequencing performed by Prof. Stefan Niemann and Dr. Thomas A. Kohl. I would also like to thank Prof. Thomas Rattei and Dr. Javier Geijo at the University Vienna (Vienna, Austria) for their genome analyses. Furthermore, I want to thank our laboratory collaborating colleagues of the University of Southampton (Southampton, United Kingdom) managed by Prof. Ian Clarke for the shuttle plasmid vector construction and plasmid DNA sequence analyses.

Lastly, sincere thanks are given to my friends and family supporting me not just during this work, but also during my whole studies at the University of Lübeck. As always in scientific research or even in life, there are highs and lows, therefore I was deeply grateful for their encouragement and support.